



# LUND UNIVERSITY

## Application of Texture Analysis to Functional Pulmonary CT Data

Meier, Arndt; Farrow, Catherine; Harris, Benjamin; King, Gregory; Jones, Alan

*Published in:*  
Computerized Medical Imaging and Graphics

*DOI:*  
[10.1016/j.compmedimag.2011.01.001](https://doi.org/10.1016/j.compmedimag.2011.01.001)

2011

[Link to publication](#)

*Citation for published version (APA):*  
Meier, A., Farrow, C., Harris, B., King, G., & Jones, A. (2011). Application of Texture Analysis to Functional Pulmonary CT Data. *Computerized Medical Imaging and Graphics*, 35(6), 438-450.  
<https://doi.org/10.1016/j.compmedimag.2011.01.001>

*Total number of authors:*  
5

### General rights

Unless other specific re-use rights are stated the following general rights apply:  
Copyright and moral rights for the publications made accessible in the public portal are retained by the authors and/or other copyright owners and it is a condition of accessing publications that users recognise and abide by the legal requirements associated with these rights.

- Users may download and print one copy of any publication from the public portal for the purpose of private study or research.
- You may not further distribute the material or use it for any profit-making activity or commercial gain
- You may freely distribute the URL identifying the publication in the public portal

Read more about Creative commons licenses: <https://creativecommons.org/licenses/>

### Take down policy

If you believe that this document breaches copyright please contact us providing details, and we will remove access to the work immediately and investigate your claim.

LUND UNIVERSITY

PO Box 117  
221 00 Lund  
+46 46-222 00 00

Elsevier Editorial System(tm) for Computerized Medical Imaging and Graphics  
Manuscript Draft

Manuscript Number:

Title: Application of Texture Analysis to Functional Pulmonary CT Data

Article Type: Full Length Article

Section/Category:

Keywords: texture analysis, computed tomography, asthma, COPD, lung ventilation

Corresponding Author: Dr Arndt Meier,

Corresponding Author's Institution: University of Sydney

First Author: Arndt Meier

Order of Authors: Arndt Meier; Catherine Walsh; Benjamin E Harris; Gregory G King; Allan Jones,  
Dr

Manuscript Region of Origin:

Abstract: Abstract

It is demonstrated that textural parameters calculated from functional pulmonary CT data have the potential to provide a robust and objective quantitative characterisation of inhomogeneity in lung function and classification of lung diseases in routine clinical applications. Clear recommendations are made for optimum data preparation and textural parameter selection.

A new set of platform-independent software tools are presented that are implemented as plug-ins for ImageJ. The tools allow segmentation and subsequent histogram-based and grey-level co-occurrence matrix based analysis of the regions of interest. The work-flow is optimised for use in a clinical environment for the analysis of transverse Computed Tomography (CT) scans and lung

ventilation scans based on SPECT. Consistency tests are made against other texture analysis plug-ins and simulated lung CT data. The same methods are then applied to patient data consisting of a healthy reference group and one patient group each who suffered from asthma, chronic obstructive pulmonary disease (COPD), and COPD plus lung cancer. The potential for disease classification based on computer analysis is evaluated.

## Application of Texture Analysis to Functional Pulmonary CT Data

Arndt Meier<sup>a</sup>, Catherine Walsh<sup>b,c,d</sup>, Benjamin E. Harris<sup>b,c,d</sup>, Gregory G.King<sup>b,c,d</sup>, and Allan Jones<sup>a</sup>

a) Australian Key Centre for Microscopy and Microanalysis, The University of Sydney, Sydney 2006, NSW, Australia, email: [a.meier@usyd.edu.au](mailto:a.meier@usyd.edu.au) (*corresponding author*)

b) Department of Respiratory Medicine, Royal North Shore Hospital, St Leonards NSW 2065

c) Woolcock Inst. of Medical Research, 431 Glebe Point Road, Glebe, NSW 2037

d) Northern Clinical School, Faculty of Medicine, University of Sydney, Sydney, 2006

1 **Abstract**  
2  
3

4 It is demonstrated that textural parameters calculated from functional pulmonary CT data  
5  
6 have the potential to provide a robust and objective quantitative characterisation of  
7  
8 inhomogeneity in lung function and classification of lung diseases in routine clinical  
9  
10 applications. Clear recommendations are made for optimum data preparation and textural  
11  
12 parameter selection.  
13  
14

15  
16 A new set of platform-independent software tools are presented that are implemented as plug-  
17  
18 ins for ImageJ. The tools allow segmentation and subsequent histogram-based and grey-level  
19  
20 co-occurrence matrix based analysis of the regions of interest. The work-flow is optimised  
21  
22 for use in a clinical environment for the analysis of transverse Computed Tomography (CT)  
23  
24 scans and lung ventilation scans based on SPECT. Consistency tests are made against other  
25  
26 texture analysis plug-ins and simulated lung CT data. The same methods are then applied to  
27  
28 patient data consisting of a healthy reference group and one patient group each who suffered  
29  
30 from asthma, chronic obstructive pulmonary disease (COPD), and COPD plus lung cancer.  
31  
32 The potential for disease classification based on computer analysis is evaluated.  
33  
34  
35  
36  
37  
38  
39  
40  
41  
42  
43  
44  
45  
46  
47  
48

49 **KEYWORDS:**  
50

51  
52 texture analysis, computed tomography, asthma, COPD, lung ventilation  
53  
54  
55  
56  
57  
58  
59  
60  
61  
62  
63  
64  
65

## 1. Introduction

Close to 10 percent of the world population are suffering from chronic lung diseases. The two most common categories, which account for 7.7%, are asthma and chronic obstructive pulmonary disease (COPD).

According to World Health Organisation (WHO) estimates, 300 million people suffer from asthma and 255 000 people died of asthma in 2005 (WHO, 2008a) and an increase of 20% is expected over the next 10 years. Asthma is the most common chronic disease among children.

It is characterised by episodic airway narrowing that occurs on exposure to stimuli, such as exercise, dust, pollens and cold air. Asthmatic lungs are characterised by inhomogeneous ventilation when studied by pulmonary function techniques or by imaging methods. The severity of the inhomogeneity, measured by pulmonary function, is strongly related to the sensitivity of airways to inhalants, i.e. dust, pollens etc. Thus characterisation of the topographical pattern of ventilation in asthmatic lungs is important

The WHO estimates (2007), currently 210 million people suffer from chronic obstructive pulmonary disease (COPD) with 3 million people dying of COPD in 2005 (WHO, 2008b).

COPD is a chronic disease that is caused predominantly by tobacco smoking in western countries. COPD causes lung destruction, known as emphysema, and diseases of small and large airways, which result in cough, mucous production and airway narrowing with resultant breathlessness during exertion.

Single-photon emission computed tomography (SPECT) ventilation scanning (Petersson *et al.*, 2007) using Technetium-99 (Technegas<sup>TM</sup>), is a three dimensional imaging technique used routinely in clinical nuclear medicine for diagnosis of diseases such as pulmonary embolism, when combined with imaging of blood flow (Harris *et al.*, 2007). Ventilation scans, however, have been adapted for studies of ventilation in airways disease (King *et al.*, 1997 and 1998,

1 Downie *et al.*, 2007). SPECT imaging offers the potential to characterise the topographical  
2  
3 distribution of ventilation so that inhomogeneity can be quantified at the regional level (Xu *et*  
4  
5 *al.*, 2001, Venegas *et al.*, 2005). Combining imaging information with the pulmonary function  
6  
7 measures of inhomogeneity will provide important information about the ventilatory  
8  
9 abnormalities in asthma and COPD (Tgavalekos *et al.*, 2007, Berend *et al.*, 2008). However,  
10  
11 suitable methods for quantifying the distribution of ventilation from SPECT data have not  
12  
13 been determined.  
14  
15  
16

17  
18 In this study, we investigate several potentially useful methods of quantifying the distribution  
19  
20 of ventilation from SPECT ventilation data using both simulated SPECT data and data from  
21  
22 well-described clinical groups. The new technique is based on texture analysis and can  
23  
24 provide an objective indicator of abnormal lung conditions.  
25  
26  
27  
28  
29  
30

## 31 **2. Methods**

32  
33  
34  
35 We developed new techniques for multiple 3D texture analysis and conventional 3D image  
36  
37 analysis of clinical SPECT data of volumes representing lung tissue as identified from co-  
38  
39 registered CT scans that were obtained at the time of the SPECT.  
40  
41

42  
43 The new technique uses the anatomical CT to define the lung outlines, co-registers these with  
44  
45 the functional SPECT data and performs an image analysis on the voxels of the SPECT thus  
46  
47 defined as representing lung tissue. The image analysis comprises a traditional direct analysis  
48  
49 of the grey levels in the SPECT slices and a texture parameters analysis derived from grey-  
50  
51 level co-occurrence matrices (GLCM) (Haralick, *et al.*, 1973, Choi, 2006).  
52  
53  
54  
55  
56  
57

### 58 **2.1 Simulation data**

59  
60  
61  
62  
63  
64  
65

1 We created a series of SPECT-V data sets based on simulated data to validate the software.

2  
3 The lung phantom used in the construction of the model was based upon X-ray computed  
4 tomography (CT) data from a male of height 178 cm, weighing 70 kg (Zubal *et al.*, 1994) in  
5 supine position, who was chosen for his similarity to the dosimetry standard mathematical  
6 phantom. The Monte Carlo simulation package used for this work was the Photon History  
7 Generator (Lewellen *et al.*, 1988, Haynor *et al.*, 1991), which models the emission, scatter and  
8 attenuation of photons in a heterogeneous phantom, followed by the photons' subsequent  
9 collimation and detection (Chicco *et al.*, 2001).

10  
11 Simulations were performed for a 23.6-mm-thick parallel-hole collimator, using a 32.5-cm  
12 radius of rotation. The isotope modelled was Tc99, collected with a symmetric 20% energy  
13 window centred around 140 keV into a 128×128 matrix with 120 views at equal angular  
14 spacing around 360°, resulting in 5 million counts total when no defects were present. Pixel  
15 resolution was 2.5mm/pixel. To test for any dependence on brightness changes we repeated  
16 two simulations with 9 million counts. These settings were chosen to closely mimic typical  
17 clinical settings when collecting SPECT-V data (similar contrast, spatial resolution and signal  
18 to noise).

19  
20 A series of studies were performed in four groups, distinguished by the size of individual  
21 defects, to simulate the effects of non-ventilated lung tissue. Defects in groups 1–4 were  
22 1x1x1 pixels (15 mm<sup>3</sup>), 2x2x2 pixels (125 mm<sup>3</sup>), 3x3x3 pixels (422 mm<sup>3</sup>) and 4x4x4 pixels  
23 (1000 mm<sup>3</sup>) in size, respectively. These were distributed uniformly throughout both lung  
24 halves in a random manner. Within each group, the amount of lung tissue involved in defects  
25 varied from 0% (normal) up to 40% in steps of 5%, giving 9 studies in each group.

26  
27 These simulated lung data sets were then subjected to normal clinical processing. Lungs  
28 were reconstructed at the same resolution as routine SPECT data (128 slices with 128x128  
29 pixels, voxel size 4.664mm<sup>3</sup>). The lung outlines were known from the original phantom and  
30  
31  
32  
33  
34  
35  
36  
37  
38  
39  
40  
41  
42  
43  
44  
45  
46  
47  
48  
49  
50  
51  
52  
53  
54  
55  
56  
57  
58  
59  
60  
61  
62  
63  
64  
65



1 converted to a binary mask which was then subjected to 2 iterations with the standard ImageJ  
2  
3 erosion operation using a count of 3 (minimum 3 of the nearest neighbour pixels need to be  
4  
5 background pixels for the present pixel to be eroded).  
6  
7  
8  
9

## 10 11 **2.2 Clinical data**

12  
13  
14 Three groups of patients were studied to evaluate the applicability of the new methods. Five  
15  
16 patients had asthma (data set A), and 10 current or ex-smokers that had either diagnosed  
17  
18 COPD (data set C) or were being evaluated for treatment of lung cancer (PELICAN<sup>1</sup> data set)  
19  
20 who had a wide range of severity of COPD, and scans from 5 patients who underwent lung  
21  
22 scanning for suspected pulmonary embolism but who were considered to have normal lung  
23  
24 scans on routine clinical assessment (data set N).  
25  
26  
27  
28

29  
30 All subjects inhaled Technegas as the ventilation imaging agent. Patients had scans according  
31  
32 to the standard clinical protocol whereby Technegas was inhaled from the Technegas  
33  
34 generator by 1-2 deep inspirations followed by a breath hold to maximise Technegas particle  
35  
36 deposition.  
37  
38  
39

40  
41 Subjects had a ventilation SPECT scan and a CT scan acquired by a dual-detector variable  
42  
43 angle hybrid SPECT/CT system (Phillips SKYLight and Picker PQ5000 CT). All SPECT  
44  
45 studies were acquired using a 128 x 128 matrix, at 15 seconds per stop with 3 degree steps  
46  
47 over 360 degrees. Low-dose CT was performed using non-contrast (30mA, 10kVp, pitch 1.5,  
48  
49 slice thickness 4mm). Study was acquired during tidal breathing. CT images are reconstructed  
50  
51 using a 512 x 512 matrix with a smooth algorithm.  
52  
53  
54

55  
56 Spirometry, including the predicted forced expiratory volume during one second (FeV1), was  
57  
58 obtained in all groups except the normal group, using standard methods in the lung function  
59

---

60 <sup>1</sup>PELICAN study: Predicting Exercise tolerance and Lung function using Imaging in patients  
61 undergoing CANcer Surgery, Royal North Shore Hospital, internal study, 2007.  
62  
63  
64  
65

1 laboratory.  
2  
3  
4  
5  
6

### 7 **2.3 Software** 8 9

10 Custom plug-ins were developed for ImageJ (Rasband, 1997-2008) to read and write CT data  
11 routinely stored in Interfile data format (Craddock et al., 1989). Segmentation of the lungs in  
12 the CT datasets is done with a custom written plug-in “Extract\_Lungs”, which was more  
13 efficient than existing segmentation plug-ins (Parker, 2008, Castleman, 2005). Segmentation  
14 uses an edge-following algorithm that stays between an upper and lower grey-value threshold.  
15  
16  
17  
18  
19  
20  
21

22 If the initial seed-point falls outside the thresholds, a new seed-point is automatically  
23 determined from a search towards the median point of the previous slice and an outward spiral  
24 from there if that fails.  
25  
26  
27  
28  
29

30 Up to 5 regions of interest per slice are supported which are categorised as belonging to either  
31 the left or right lungs. A custom-built ROI manager allows superimposition of the ROIs onto  
32 SPECT ventilation data. The identified volumes are analysed for total area, mean, median,  
33 modal, minimum, and maximum grey values, kurtosis, integrated optical density (IOD), and  
34 histogram. Weighted means are calculated for left, right and total lung.  
35  
36  
37  
38  
39  
40  
41  
42

43 Anatomical CT data were registered to corresponding functional data (SPECT) with the  
44 ImageJ plug-in Align3\_TP (Parker, 2008) with all parameters left to their default values. The  
45 outlines of the registered lung mask were then auto-detected with our segmentation algorithm  
46 resulting in ImageJ standard ROIs (regions of interest). Our modified ROI manager limits all  
47 subsequent analysis to within the defined ROIs.  
48  
49  
50  
51  
52  
53  
54

55 From these ROIs that represent the total lung volume, GLCMs are calculated for the x, y, z,  
56 and invariant orientation for a set of up to 5 chosen distances. These are then subjected to  
57 standard texture analysis. We verified the correct implementation of the GLCM algorithm by  
58  
59  
60  
61  
62  
63  
64  
65

1 comparing results from an independently written plug-in [Cabrera, 2005], which calculates 4  
2  
3 of the 12 textural features we determine, and found both to be consistent.  
4  
5

6 Our methods are based on software that is easily available, widely used, modular in design,  
7  
8 open source and not limited to a specific operating system. ImageJ (Rasband, 1997-2008),  
9  
10 Abramoff *et al.*, 2004, Burger & Burge, 2008) fulfils all these criteria perfectly. And more so,  
11  
12 there is a very large collection of plug-ins publicly available  
13  
14 (http://rsb.info.nih.gov/ij/plugins/). The code used in this study is available from the author.  
15  
16  
17  
18  
19  
20  
21

## 22 **2.4 Analysis**

23  
24

25 In both the simulated and the clinical data the volumes representing lung tissue were  
26  
27 identified as described above. All voxels outside the eroded ROIs were excluded from the  
28  
29 analysis. Note that lung tissue outlines were registered to the reconstructed SPECT data, thus  
30  
31 avoiding any interpolation in the SPECT data set.  
32  
33  
34

35 All SPECT data sets, simulated and clinical, were prepared in two parallel streams: *CS*  
36  
37 (contrast stretched) and *HM* (histogram matched). The contrast stretched data set was created  
38  
39 by first stretching the contrast within the 16-bit grey-levels image stack using the stack  
40  
41 histogram (built-in ImageJ function) and then converting the image stack to an 8-bit grey-  
42  
43 level image stack. The latter step used an improved version of the ImageJ Stack Converter  
44  
45 that uses the stack histogram as opposed to the histogram of the current slice and allows to  
46  
47 fold a set percentage of hot pixels into the highest remaining histogram channel. We chose the  
48  
49 0.02% brightest non-background pixels to be treated as hot pixels.  
50  
51  
52  
53  
54

55 The histogram-matched data set used the histogram from the best ventilated simulated lung as  
56  
57 the reference histogram after smoothing it twice with a Gaussian filter of 5 histogram  
58  
59 channels width. This histogram compared well with histograms obtained from patients with  
60  
61  
62  
63  
64  
65

1 normal lung function. The histogram matcher we wrote uses the stack histogram and can  
2  
3 directly map a 16-bit image stack onto an 8-bit reference histogram thus considerably  
4  
5 reducing channel pile-up effects commonly encountered when first converting from 16-bit to  
6  
7 8-bit and then again from 8-bit to 8-bit reference histogram.  
8  
9

10 The 'extracted lungs' as defined by sets of ROIs were then analysed in two steps. The normal  
11  
12 grey value analysis calculated the total lung volume in voxels, the ventilated volume, the  
13  
14 minimum, mean, modal, median and maximum grey values, IOD, contrast, histogram, and  
15  
16 Kurtosis on a per-ROI basis. Mean values weighted by ROI area were calculated for left,  
17  
18 right, and total lung.  
19  
20  
21  
22  
23

24 A voxel was considered to represent ventilated lung tissue if it had a grey value larger than  
25  
26 20% of the histogram maximum. To minimise the impact of any erratic hot pixels, the  
27  
28 histogram maximum was calculated from the 97% level assuming that the histogram above  
29  
30 97% drops with a slope of -0.5. In this work we only report the results for total lungs, but it is  
31  
32 noted that the software reports more details where this may be of interest.  
33  
34  
35

36 The second step of the analysis created 8-bit grey-level co-occurrence matrices (GLCMs)  
37  
38 from all the ROIs of any one lung for 5 distances each: 1, 2, 4, 8, and 12 pixels (4.7, 9.3, 18.7,  
39  
40 37.3, 56.0mm) and for 4 direction pairs each: X (left->right, right->left), Y (top->bottom,  
41  
42 bottom->top), Z (up->down, down->up) and I (invariant, combining X, Y, and Z). The  
43  
44 invariant matrix we chose gives equal weight to each valid voxel pair and may at times differ  
45  
46 from a mean over the X, Y, and Z matrices as individual matrices may not have the exact  
47  
48 same number of voxel pairs. From these GLCMs twelve texture features were calculated as  
49  
50 listed in appendix A (Haralick *et al.*, 1973, Haralick 1979, Choi, 1996).  
51  
52  
53  
54  
55  
56  
57  
58  
59

### 60 **3. Results**

61  
62  
63  
64  
65

### 3.1 Results from the phantom study

The texture parameters calculated from the simulated lungs show a number of correlations with the size of the defects and the total non-ventilated volume (NVV). Figure 1 illustrates this for the example of the textural parameter TC18 (coefficient of variation) and simulated defect sizes of 3x3x3 pixels. For all GLCM distances and defect sizes the parameter TC18 increases steadily with increasing NVV and more rapidly so for larger defects.

No significant differences were found between results obtained from X, Y, and Z GLCMs.

Hence only the invariant GLCMs have been studied further. For all 12 textural parameters studied we found under all conditions that the functions such as in Figure 1 are smooth and steady and that different distances in GLCM calculation result in slightly shifted versions of the same shape but that in no case does the graph of one distance cross the graph of another distance for otherwise identical settings. On the contrary, we often saw that graphs for different distances were almost undistinguishable from one another. Consequently the data from all distances were pooled into one; thus reducing the complexity of the results presented. Notwithstanding this, it is noted, that TC9 and TC30 were somewhat more sensitive to NVV changes at shorter distances and that TC2 showed no dependence on NVV but gave significantly different results for different distances.

For clarity only the relative changes in textural parameters between the lowest and highest NVV studied are reported, because the functions change smoothly with NVV and in-between values do not add much to the discussion.

Table 1 lists the relative changes in the textural parameters calculated in response to a 40% drop in ventilated lung volume. Some textural parameters are more sensitive to the changes in ventilated volume than others as can be seen from Table 1 (rows 6 and 11 “*mean*”). Also, they are typically stronger in the contrast-stretched data set (*cs*, row 6) as compared to the

1 histogram-matched data set (*hm*, row 11).  
2  
3

4 The results from a sensitivity test to brightness changes are shown in Table 2. We repeated the  
5 simulation for the “worst” lung with a higher activity such that after adding the defects it  
6 resulted in the same IOD as the perfectly ventilated simulated lung. Insensitivity to brightness  
7 changes would allow the direct comparison of textural parameters derived from studies that  
8 use different gamma counts. Note that rows 2 and 3 in Table 2 correspond to rows 5 and 10 in  
9 Table 1 (10 mm), respectively, but the percentage changes are expressed relative to the values  
10 in Table 1. It is noted that the sign of all values in Table 2 act in such a way as to reduce the  
11 sensitivity of the textural parameters.  
12  
13  
14  
15  
16  
17  
18  
19  
20  
21

22 In the context of our work a good textural parameter is one that is sensitive to changes in  
23 NVV or defect-size and that is at the same time insensitive to changes in brightness. With this  
24 in mind we can group the textural parameters investigated into robust, intermediate and poor  
25 performers:  
26  
27  
28  
29  
30  
31

### 32 **Robust textural parameters:**

33  
34  
35  
36  
37  
38  
39  
40 TC13/TC31 Variance/Mean ratio: provides a solid signal of 22% change in the parameter  
41 value for a 40% change in NVV while its dependence on brightness doubling is only small  
42 (1.5%). The sensitivity is somewhat poorer for smaller defects.  
43  
44

45  
46  
47  
48 TC30 Local homogeneity: provides still a good signal of 10.5% change for a 40% drop in  
49 NVV but is more sensitive to brightness changes than the TC13/TC31 ratio (2.9%).  
50

51  
52  
53 TC18 Coefficient of Variation: provides a very strong signal of 77% for large defects and a  
54 still strong signal of 22% for small defects. It has a moderate dependence on brightness  
55 changes (10.8% simulating large defects). However, correlation with clinical data discussed  
56 below is excellent.  
57  
58  
59  
60  
61  
62  
63  
64  
65

1  
2  
3  
4  
5  
6  
7  
8  
9  
10  
11  
12  
13  
14  
15  
16  
17  
18  
19  
20  
21  
22  
23  
24  
25  
26  
27  
28  
29  
30  
31  
32  
33  
34  
35  
36  
37  
38  
39  
40  
41  
42  
43  
44  
45  
46  
47  
48  
49  
50  
51  
52  
53  
54  
55  
56  
57  
58  
59  
60  
61  
62  
63  
64  
65

**Textural parameters with intermediate performance:**

TC1 Angular second moment: provides high sensitivity (>68%) to changes in NVV, but unfortunately it is also very sensitive to brightness changes.

TC2 and TC2: Difference and inverse difference moment: show a modest sensitivity for short distances and small-sized defects but are insensitive at larger pixel distances as well as for larger defect sizes. However, they may be used successfully in conjunction with other parameters to decide whether the effective size distribution of the non-ventilated volumes is small or large.

TC9 Correlation: The theoretical study shows a reasonable sensitivity of around 20% to changes twice that large in NVV but also a relatively high sensitivity to brightness changes. In the clinical studies discussed below this parameter did not convince and is outperformed by others.

**Textural parameters with poor performance:**

TC7, TC4, TC13, TC31, TC21, and TC23: These parameters suffer either from a lack of sensitivity or high sensitivity to changes in brightness.

**Combination of textural parameters:**

The ratio of TC13/TC31 is a very good performer although neither TC13 nor TC31 are good performers. Similarly, the ratio of TC21/TC31 gives a moderately good performance.

**3.2 Results from the clinical studies**

1 Figure 2 illustrates the estimated ventilated lung volume grouped by patient group. The  
2  
3 'normal' group shows the highest ventilated volume of about 90% and the smallest variance.  
4  
5 Asthmatic lungs at baseline show a slightly lower ventilated lung volume although not  
6  
7 statistically significant from the 'normal' lungs. The remaining patient groups show significant  
8  
9 reductions in ventilated lung volume that are strongest in COPD patients. There is also a  
10  
11 higher variability in these groups.  
12  
13  
14  
15

16 Figures 3 and 4 illustrate one of the best performing textural parameters for the 5 patient  
17  
18 groups studied. Both the absolute value and the variability between different GLCM distances  
19  
20 and between patients in the 'normal' lung function group are small (Figure 3, left panel). The  
21  
22 results from COPD patients which range from a mild case (right panel, c-01) to severe (c-05)  
23  
24 show increasingly higher values.  
25  
26  
27  
28

29 The differences between using different distances in the GLCM calculations are almost within  
30  
31 the numerical precision, which was also observed in the results from the simulated data. This  
32  
33 observation holds true for all textural parameters and patient groups studied except for TC2,  
34  
35 TC9 and TC30. TC9 (Correlation) and TC30 (Local Homogeneity) lose sensitivity with  
36  
37 increasing distance between voxel pairs and better performance is achieved by only using the  
38  
39 2 shortest distances (1 and 2 pixels distance corresponding to 4.7 and 9.3mm, respectively).  
40  
41  
42  
43  
44  
45  
46  
47  
48  
49  
50  
51  
52  
53  
54  
55  
56  
57  
58  
59  
60  
61  
62  
63  
64  
65

61  
62  
63  
64  
65

62 Pooling the data from all GLCM distances<sup>2</sup> and by patient group allows us to look for disease-  
63  
64 specific differences as shown in Figure 4. While asthmatics at baseline cannot be distinguished  
65  
66 from normal lungs, they can be clearly identified after a Metacholine challenge. PELICAN  
67  
68 patients and even more so COPD patients have strongly elevated values in the coefficient of  
69  
70 variation calculated from the GLCM.

---

<sup>2</sup> Except for TC9 and TC30 which pooled only the 2 shortest distances for higher sensitivity



1 Figure 5 presents the ratio of Local Homogeneity and GLCM Mean (TC30/TC31) calculated  
2  
3 in the same way as in the previous figure. Again, values for COPD and PELICAN patients are  
4  
5 significantly higher than those for normal and asthmatic lungs. It is noted, however, that  
6  
7 asthma patients both at baseline and at Metacholine challenge give almost identical results.  
8  
9 Hence combining the information from multiple textural parameters allows to distinguish  
10  
11 between different disease classes such as asthma from COPD.  
12  
13

14  
15 A very strong correlation ( $r^2=0.955$ ) between the textural parameter Coefficient of Variation  
16  
17 (TC18) and the estimated ventilated lung volume is illustrated in Figure 6. Similarly high  
18  
19 correlations of  $r^2>0.8$  exist for textural parameters TC3, TC30, TC31, and the ratios  
20  
21 TC13/TC31 and TC21/TC31 as a function of ventilated lung volume (not illustrated). More  
22  
23 positive correlations ( $r^2>0.49$ ) are observed for textural parameters TC1, TC9, and the ratio  
24  
25 TC1/TC31.  
26  
27

28  
29 Independent spirometry data in the form of the predicted forced expiratory volume during 1  
30  
31 second (FeV1) was available for all but the 'normal' group. Again good correlations are  
32  
33 observed with several textural parameters ( $r^2>0.5$  for TC18 and TC13/TC31,  $r^2>0.4$  for TC3,  
34  
35 TC30, TC21/TC31, TC31 and TC1/TC31 and  $r^2>0.3$  for TC1, TC2 and TC9) as illustrated in  
36  
37 Figure 7 for the example of TC13/TC31.  
38  
39

40  
41 The Difference Moment (TC2) behaves differently from all other textural parameters studied.  
42  
43 It is insensitive to changes in both NVV and FeV1, but it is sensitive to the size distribution of  
44  
45 patterns in the lung. Hence the TC2 textural parameter results were prepared in a different  
46  
47 way. Instead of pooling the results from different GLCM distances, the parameter value  
48  
49 obtained with the shortest distance (1 pixel) were divided by the parameter value for the  
50  
51 second largest distance for any one lung and that we refer to as TC2<sub>d</sub> for short. Data prepared  
52  
53 in this way resulted in a positive correlation of TC2<sub>d</sub> with NVV ( $r^2=0.69$ ) and a somewhat  
54  
55 weaker correlation with FeV1 ( $r^2=0.375$ ).  
56  
57  
58  
59  
60  
61  
62  
63  
64  
65

1 All results in this section were derived from the contrast-stretched data set as it showed an  
2  
3 overall better performance than compared to results derived from the histogram-matched data.  
4  
5 It is noted that TC18, TC31 (Mean) and TC13/TC31 were indifferent to both NVV and FeV1  
6  
7 changes in the histogram-matched data set, but otherwise the same textural parameters  
8  
9 performed well as in the contrast-stretched data set. The only textural parameter that faired  
10  
11 significantly better in the histogram-matched data set was TC23 (Difference Entropy).  
12  
13  
14  
15  
16  
17  
18

#### 19 **4 Discussion**

20  
21  
22 Changes in the grey level distribution such as a shift to darker grey values – as can be  
23  
24 expected with a reduction in ventilated lung volume – is essentially removed in the histogram-  
25  
26 matched data. Hence, changes in the textural parameters that occur in the contrast-stretched  
27  
28 data set but not in the histogram-matched one are thought to be driven by histogram changes  
29  
30 while changes that occur in the histogram-matched data set are thought to be dominated by  
31  
32 changes in pattern (Table 1). Changes in the contrast-stretched data set are often a result of  
33  
34 both histogram and pattern changes.  
35  
36  
37  
38  
39

40 In an ideal system a change in brightness should not affect the textural parameters calculated  
41  
42 because the GLCMs are always normalised to an IOD of unity. However, it is noted that the  
43  
44 spatial resolution of the observation system is significantly lower than the features that cause  
45  
46 them. The effective resolution in the SPECT-V data is lower than the pixel resolution of  
47  
48 4.664mm/pxl which in turn is much coarser than the simulated small defects starting from  
49  
50 2.5mm cube side length. Due to the nature of discrete sampling – and in this case significant  
51  
52 under-sampling – of the object space and the non-linearity of the resulting effective blurring,  
53  
54 the texture parameters calculated become dependent on the total optical density and contrast  
55  
56 in the SPECT-V data sets. This effect itself is also dependent on the effective size distribution  
57  
58  
59  
60  
61  
62  
63  
64  
65

1 of the defects we seek to describe. To quantitatively describe the exact relationship is  
2  
3 mathematically complex and of limited practical use as it will vary from situation to situation.  
4  
5 Instead we seek to identify textural parameters that depend acceptably little on the variability  
6  
7 in patient data preparation.  
8  
9

10  
11 The simulated data allows to fully control the environment, to know the true size distribution  
12  
13 of the non-ventilated lung volumes, the true ventilated volume, and to vary some of these  
14  
15 parameters systematically to study its impact. However, there are also some differences and  
16  
17 limitations compared to clinical data that are undesirable. One is that the IOD of the simulated  
18  
19 SPECT-V scan drops progressively with increasing NVV due to the simplicity of the model  
20  
21 available to us.  
22  
23  
24  
25

26  
27 A patient with a smaller ventilated lung volume inhales approximately the same amount of  
28  
29 radioactivity as a patient with a larger ventilated lung volume. As a result the scan from the  
30  
31 former patient would have a larger information content<sup>3</sup> and image contrast; because the same  
32  
33 amount of activity has to squeeze into a smaller volume, a wider range of different brightness  
34  
35 values is observed. Hence a poorly ventilated *simulated* lung has a somewhat *lower*  
36  
37 information content in the simulated data in contrast to a patient with a poorly ventilated lung  
38  
39 that would result in a *higher* information content than the ideally ventilated lung. We studied  
40  
41 this behaviour by simulating one data set with a higher gamma count, which resulted in an  
42  
43 increase of 38% in information content as opposed to a 9% drop in the non-corrected  
44  
45 simulation case. Although the textural parameters are modified as a result, it does not change  
46  
47 the overall response to NVV and we were able to identify textural parameters that are little or  
48  
49 non-susceptible to this change (Table 2). This finding is also directly relevant to clinical data,  
50  
51 because any two patients with naturally differently-sized lungs that are administered the same  
52  
53 amount of Technegas will have differences in contrast and information content of the SPECT  
54  
55  
56  
57  
58  
59

---

60  
61 <sup>3</sup> We use the term information content in the strict sense of the number of grey values in an associated  
62 histogram that are non-zero.  
63  
64  
65

1 recorded. Selecting textural parameters that are insensitive to this variability in data collection  
2  
3 is an advantage in data interpretation.  
4

5  
6 Reconstructed SPECT data is routinely subjected to a rather strong smoothing filter before  
7  
8 being presented to a radiographer or other medical professional. Filtering at the RNSH  
9  
10 consists of a 9<sup>th</sup> order Butterworth filter with a cut-off of 1.2 cycles per centimetre. Since  
11  
12 texture analysis by definition looks at small differences in grey values between pairs of pixels,  
13  
14 any smoothing operation degrades the capabilities of the method for any given case. We tested  
15  
16 this expected behaviour by preparing both simulated and normal patient data with and  
17  
18 without applying the Butterworth filter and found the smoothed data set to have a poorer  
19  
20 sensitivity as manifested in smaller relative changes in textural parameters. We will report the  
21  
22 exact impact in a forthcoming separate study. In this work we only discuss reconstructed,  
23  
24 extracted lung data that has **not** been subjected to any post-filtering.  
25  
26  
27  
28  
29  
30

31 A change of distance in the calculation of the GLCMs (within reason) adds little new  
32  
33 information (Figure 1) with the exception of parameter TC2. In most cases the calculation of  
34  
35 the GLCM for only one distance seems to be sufficient. For 2 of the textural parameters  
36  
37 studied there is a better performance seen for shorter distances in the GLCM calculations  
38  
39 (TC9 and TC30). This is plausible looking at the definitions (Appendix 1). Voxel pairs that are  
40  
41 far from one another are unlikely to be highly correlated thus giving low correlation values in  
42  
43 any lung (TC9) and uniformity between them will be near the random value (TC30).  
44  
45  
46  
47

48 From the simulated data it is known that TC2<sub>d</sub> drops with increasing defect size and in the  
49  
50 patient data it drops with increasing NVV. This suggests that the average size of individual,  
51  
52 non-ventilated areas increases with the severity of the diseases studied as opposed to a mere  
53  
54 increase of number of non-ventilated areas of same size. This result is consistent with the  
55  
56 perception of the SPECT data to the human eye.  
57  
58  
59

60  
61 Several well performing textural parameters were identified that by themselves allow to  
62  
63  
64  
65

1 distinguish between a 'normal' lung and a lung that suffers from some significant medical  
2  
3 condition or disease. Combinations of textural parameters have the potential to further classify  
4  
5 abnormal lungs. For example, to distinguish between asthmatics on one hand and COPD  
6  
7 patients on the other hand one can combine the results from TC18 and the ratio TC30/TC31.  
8  
9

10 TC18 is elevated in all diseases, but the ratio TC30/TC31 does not rise significantly in  
11  
12 asthmatics while it does rise significantly in COPD patients (compare Figures 4 and 5).  
13  
14

15  
16 Correlation of several key textural parameters with the corresponding ventilated lung volume  
17  
18 are good to excellent for all patient data (Figures 6 and 7). Note that the ventilated lung  
19  
20 volume is a measure that is calculated from the original imaging data (not the GLCM), while  
21  
22 the FeV1 is a completely independent measurement. The pooling of data per disease group  
23  
24 (Figures 4 and 5) combines all patients of one disease into one - independent of the severity of  
25  
26 disease. Figures 6 and 7 on the other hand illustrate the relationship between reduced lung  
27  
28 functionality and resulting changes in derived textural parameters. It is pointed out that  
29  
30 reduced lung functionality goes along with higher heterogeneity in the SPECT data (Berend  
31  
32 *et al.*, 2008) and textural parameters that measure heterogeneity increase while parameters  
33  
34 that measure uniformity drop.  
35  
36  
37  
38  
39

40  
41 The textural parameters discussed are not all linearly independent of one another but some of  
42  
43 them have substantial correlations amongst them. (Clausi, 2008). For practical matters it is  
44  
45 desirable to identify a small number of textural parameters that give the overall best  
46  
47 classification performance.  
48  
49

50  
51 TC2, TC3, TC4 and TC30 are all measures of contrast, though with different weights. TC3  
52  
53 and TC30, which weigh values by the inverse of the contrast (homogeneity), have both shown  
54  
55 consistently better performance in all patient data and either one of these two parameters are  
56  
57 recommend for use. As TC3 and TC30 are highly correlated one should choose only one of  
58  
59 them with TC3 performing marginally better in contrast-stretched data sets and TC30 better in  
60  
61  
62  
63  
64  
65

1 histogram-matched data sets.  
2

3  
4 TC1, TC21 and TC23 are all measures of orderliness. The ratio TC21/TC31 performed best in  
5  
6 the clinical data. The GLCM Mean (TC31) reflects brightness changes between patients that  
7  
8 the contrast-stretched data set is susceptible to. Thus using textural parameter combinations  
9  
10 that involve the GLCM Mean improves correlation in several textural parameters studied. The  
11  
12 histogram-matched data set shows no correlation with TC31 and combining textural  
13  
14 parameters with TC31 carries no advantage and TC23 by itself gives the best performance in  
15  
16 the group of textural parameters that measure orderliness. The value of Entropy (TC21, TC23)  
17  
18 increases with increasing heterogeneity.  
19  
20  
21

22  
23  
24 TC9 (Correlation), TC13 (Variance), TC18 (Coefficient of Variation) and TC31 (Mean) are  
25  
26 descriptive statistics of the GLCMs and the frequency at which certain voxel *pairs* occur. The  
27  
28 combination of Variance and Mean in the Coefficient of Variation (TC18) and the Variance  
29  
30 over Mean ratio (TC13/TC31) gave excellent performance in the contrast-stretched data set  
31  
32 and is another recommended parameter for use. TC18 and the TC13/TC31 ratio are highly  
33  
34 correlated parameters. TC18 shows better correlation with ventilated lung volume and TC13/  
35  
36 TC31 shows better correlation with FeV1 but either one being a very good choice for  
37  
38 characterising the clinical data.  
39  
40  
41

42  
43  
44 GLCM Correlation (TC9) Is largely independent of the other texture measures and has the  
45  
46 potential for giving additional insight. TC9 can be calculated for increasingly larger voxel  
47  
48 distances and the size at which the value suddenly decreases is a measure for the size of  
49  
50 definable objects in the original image data. However, we could not identify any 'sharp' drops  
51  
52 but only gradual changes with the clinical data, suggesting that there is a broad size  
53  
54 distribution of objects which makes this approach less powerful. Simply comparing the  
55  
56 differences in Correlation values between the shortest and longest distance studied with  
57  
58 ventilated lung volume resulted in a modest correlation ( $r^2=0.41$ ).  
59  
60  
61  
62  
63  
64  
65

1 It is noted that the best correlations between textural parameters and ventilated lung volume  
2  
3 were achieved with a linear regression while correlation with FeV1 gave consistently better  
4  
5 results using a logarithmic correlation function.  
6  
7

8  
9 Summed up the following 3 recommendations can be made for the analysis of pulmonary  
10  
11 SPECT-V data.  
12

- 13  
14 1) Texture analysis sensitivity is maximised by preparing SPECT data in an unfiltered,  
15  
16 contrast-stretched way, as opposed to filtered or histogram-matched.  
17  
18
- 19  
20 2) The choice of voxel pair distance in the GLCM calculation is non-critical. With  
21  
22 present spatial resolution in SPECT data 1, 2, or 3 pixel distances are good choices  
23  
24 that can also be pooled to improve statistics.  
25  
26
- 27  
28 3) Amongst the many textural parameters studied one each should be chosen from 3  
29  
30 different groups of parameters to balance the capability to characterise with the  
31  
32 computational effort involved. These are the textural parameters TC18 or the ratio  
33  
34 TC13/TC31 from the descriptive statistics group, the parameter TC3 or TC30 from the  
35  
36 contrast group and the parameter ratio TC21/TC31 in the orderliness group.  
37  
38  
39

40 Application of the new software package is not limited to pulmonary studies – in fact it may  
41  
42 also be applied to other organs or to completely different fields such as material sciences or  
43  
44 mineralogy. However, in its present form the software package is optimized to the work-flow  
45  
46 of studying lungs in a clinical scenario.  
47  
48  
49  
50  
51  
52  
53

## 54 **Summary**

55  
56

57 It has been demonstrated that a textural parameter analysis of functional pulmonary CT data  
58  
59 has the potential to provide a robust and objective quantitative characterisation of  
60  
61  
62  
63  
64  
65

1 inhomogeneity in lung function and classification of lung diseases with application in routine  
2  
3 clinical applications and national screening programmes. The new methods applied to SPECT  
4  
5 lung ventilation scans are capable of distinguishing between different types of diseases.  
6  
7 Strong correlations between key textural parameters and independent lung function data such  
8  
9 as the FeV1 suggest that a quantitative description of the severity of diseases such as asthma  
10  
11 or COPD by means of derived texture parameters is viable. Clear recommendations have been  
12  
13 made for optimum data preparation and textural parameter selection. In a forthcoming study  
14  
15 we plan to use data from larger numbers of patients and additional spirometry data to further  
16  
17 refine the methods.  
18  
19  
20  
21  
22  
23  
24  
25

## 26 **Acknowledgements**

27  
28 This work is supported by the Australian Research Council through the ARC Linkage Project  
29  
30 LP0562715. The authors are grateful for scientific and technical input and support from the  
31  
32 Australian Microscopy & Microanalysis Research Facility (AMMRF) node at  
33  
34 the University of Sydney. We also like to thank the staff at the Royal North Shore Hospital  
35  
36 that helped in the data collection and the volunteer patients that participated in this study. In  
37  
38 particular we like to thank Peter Chicco, Department of Biomedical Engineering, who  
39  
40 provided the lung simulations, Dale and Elizabeth Bailey, Department of Nuclear Medicine,  
41  
42 for discussion and data conversion.  
43  
44  
45  
46  
47  
48

49  
50 We like to thank Wayne Rasband and all other developers that made contributions to ImageJ  
51  
52 and its plug-ins for sharing their work freely with other researchers (Rasband, 1997-2008,  
53  
54 Abramoff *et al.*, 2004) – without them our work would have been much harder. Part of the  
55  
56 software presented here started their development based on other publicly available plug-ins  
57  
58 that are accessible through the ImageJ web page (Rasband,1997-2008, Castleman, 2005,  
59  
60  
61  
62  
63  
64  
65



1 Miller, 2002).  
 2  
 3  
 4  
 5

6 **References**

- 7 Abramoff, MD, Magelhaes, PJ, Ram, SJ, Image Processing with ImageJ, Biophotonics  
 8 International (2004), **11**(7):36-42  
 9  
 10 Berend N, Salome CM, King GG, Mechanisms of airway hyper-responsiveness in asthma.  
 11 Respirology (2008), **13**(5):624-631  
 12  
 13 Burger W and Burge MJ, Digital Image Processing - An Algorithmic Approach using Java.  
 14 Springer-Verlag, New York (2008). ISBN 978-1-84628-379-6, [www.imagingbook.com](http://www.imagingbook.com)  
 15  
 16 Cabrera JE, “GLCM\_Texture” plug-in for ImageJ, (2005), <http://rsb.info.nih.gov/ij/plugins/>  
 17  
 18 Castleman M, “Cell\_outliner” plug-in for ImageJ ([m@mlcastle.net](mailto:m@mlcastle.net)), Columbia University  
 19 (2005) <http://rsb.info.nih.gov/ij/plugins/cell-outliner.html>  
 20  
 21 Chicco P, Magnussen JS, Mackey DW, Bush V, Emmett L, Storey G, Bautovich G, and Wall  
 22 H van der, SPET of a computerised model of diffuse lung disease, Eur.J.Nuc.Med (2001),  
 23 **28**(2):150-154  
 24  
 25 Choi HK, New Methods for Image Analysis of Tissue Sections. PhD thesis, Uppsala  
 26 University, Sweden (1996), ISBN 91-554-3829-6  
 27  
 28 Clausi DA, An analysis of co-occurrence texture statistics as a function of grey level  
 29 quantization. Can. J. Remote Sensing, (2002), **28**(1):45–62  
 30  
 31 Craddock TD, Bailey DL, Hutton BF, Conninck F De, Busemann-Sokole E, Bergmann H, and  
 32 Noelpp U, A standard protocol for the exchange of nuclear medicine image files.  
 33 NucMedComm (1989), **10**:703-713  
 34  
 35 Downie SR, Salome CM, Verbanck S, Thompson BR, Berend N and King GG, Ventilation  
 36 heterogeneity is a major determinant of airway hyperresponsiveness in asthma, independent  
 37 of airway inflammation. Thorax (2007), **62**:684-689  
 38  
 39 Haralick RM, Shanmugam K, and Dinstein I, Textural features for image classification. IEEE  
 40 Transactions on Systems, Man, and Cybernetics (1973), SMC-**3**(6):610-621  
 41  
 42 Haralick RM, Statistical and structural approaches to texture. Proceedings of the IEEE 67  
 43 (1979), **5**:786-804  
 44  
 45 Harris BE, Bailey D, Miles S, Bailey E, Rogers K, Roach P, Thomas P, Hensley M, and King  
 46 GG, “Objective analysis of tomographic ventilation perfusion scintigraphy in pulmonary  
 47 embolism”, Am. J. Respir. Crit. Care Med. , March 15, 2007  
 48  
 49 Haynor DR, Harrison RL, Lewellen TK, The use of importance sampling techniques to  
 50 improve the efficiency of photon tracking in emission tomography simulations. Med Phys  
 51 (1991), **18**:990–1001  
 52  
 53 King GG, Eberl S, Salome CM, Meikle SR, and Woolcock AJ, Airway closure measured by a  
 54 Technegas bolus and SPECT. Am.J.Respir.Crit.CareMed. (1997) **155**:682–688  
 55  
 56 King GG, Eberl S, Salome CM, Young IH, and Woolcock AJ, Differences in airway closure  
 57 between normal and asthmatic subjects measured with single-photon emission computed  
 58 tomography and technegas. Am.J.Respir.Crit.CareMed. (1998), **158**:1900–1906.  
 59  
 60 Lewellen TK, Anson CP, Haynor DR, Design of a simulation system for emission  
 61  
 62  
 63  
 64  
 65

1 tomographs. *J Nucl Med* (1988), **29**:871  
 2  
 3 Miller M, “Segmenting\_Assistant”, plug-in for ImageJ, (2002) mmiller3@iupui.edu,  
 4 <http://rsb.info.nih.gov/ij/plugins/index.html>  
 5  
 6 Parker JA, Align3\_TP: stack alignment plug-in for ImageJ, J.A.Parker@IEEE.org (version  
 7 25/Mar/2008), <http://www.med.harvard.edu/JPNM/ij/plugins/Align3TP.html>  
 8  
 9 Petersson J, Sánchez-Crespo A, Larsson SA and Mure M, Physiological imaging of the lung:  
 10 single-photon-emission computed tomography (SPECT). *J Appl Physiol* (2007) **102**:468-476  
 11  
 12 Rasband, W.S., ImageJ, U. S. National Institutes of Health, Bethesda, Maryland, USA,  
 13 <http://rsb.info.nih.gov/ij/>, 1997-2008.  
 14  
 15 Tgavalekos NT, Musch G, Harris RS, Vidal Melo MF, Winkler T, Schroeder T, Callahan R,  
 16 Lutchen KR and Venegas JG, Relationship between airway narrowing, patchy ventilation and  
 17 lung mechanics. *Eur Respir J* (2007), **29**:1174–1181  
 18  
 19 Venegas JG, Schroeder T, Harris S, Winkler RT, and Vidal Melo MF, The distribution of  
 20 ventilation during bronchoconstriction is patchy and bimodal: A PET imaging study.  
 21 *Respiratory Physiology & Neurobiology* (2005) **148**:57–64  
 22  
 23 WHO World Health Organisation, 2008a, <http://www.who.int/respiratory/asthma/en/>  
 24  
 25 WHO World Health Organisation, 2008b, <http://www.who.int/respiratory/copd/en/>  
 26  
 27 Xu J, Moonen M, Johansson Å, Gustafsson A, and Bake B, Quantitative analysis of  
 28 inhomogeneity in ventilation SPET. *Eur J Nucl Med* (2001) **28**:1795–1800  
 29  
 30 Zubal IG, Harrell CR, Smith EO, Rattner Z, Gindi G, Hoffer PB, Computerized three-  
 31 dimensional segmented human anatomy. *Med Phys* (1994), **21**:299–302  
 32  
 33  
 34  
 35  
 36  
 37  
 38  
 39  
 40  
 41  
 42  
 43  
 44  
 45  
 46  
 47  
 48  
 49  
 50  
 51  
 52  
 53  
 54  
 55  
 56  
 57  
 58  
 59  
 60  
 61  
 62  
 63  
 64  
 65

## Appendix A: Definition of textural features from the co-occurrence matrix

A co-occurrence matrix  $P(i,j|d,\theta)$  (PM for short) contains the probability that the grey level  $i$  occurs at a distance  $d$  in direction  $\theta$  from a pixel with grey value  $j$ .  $N$  is the size of the co-occurrence matrix ( $N=256$  in this study). Integrated sums are calculated from the matrix variance. We further define the vertical ( $p_x(i)$ ), horizontal ( $p_y(i)$ ), minor diagonal ( $p_{x-y}(k)$ ) sums, the vertical ( $\mu_x$ ) and horizontal ( $\mu_y$ ) mean, and the variance of the vertical ( $V_x$ ) and horizontal ( $V_y$ ) directions (Choi, 1996). Note that the GLCM mean is distinct from the mean grey value of the original image because it is weighted by the frequency of occurrence *in combination with* a certain neighbour pixel value.

$$P_x(i) = \sum_{j=0}^{N-1} PM, \quad P_y(i) = \sum_{i=0}^{N-1} PM, \quad P_{x-y}(k) = \sum_{i=0, |i-j|=k}^{N-1} \sum_{j=0}^{N-1} PM, \quad \mu_x = \sum_i i P_x(i),$$

$$\mu_y = \sum_j j P_y(j), \quad V_x = \sum_i (i - \mu_x)^2 P_x(i), \quad V_y = \sum_j (j - \mu_y)^2 P_y(j)$$

TC\_1 Angular Second Moment  $\sum_{i=0}^{N-1} \sum_{j=0}^{N-1} PM^2$

TC\_2 Difference Moment or GLCM Contrast  $\sum_{i=0}^{N-1} \sum_{j=0}^{N-1} (i-j)^2 PM$

TC\_3 Inverse Difference Moment,  $\sum_{i=0}^{N-1} \sum_{j=0}^{N-1} (1+(i-j)^2)^{-1} PM$

TC\_4 Diagonal Moment,  $\sum_{i=0}^{N-1} \sum_{j=0}^{N-1} \sqrt{0.5(i-j)} PM$

TC\_7 Inertia,  $\sum_{n=0}^{N-1} n^2 \left( \sum_{i=0, |i-j|=n}^{N-1} \sum_{j=0}^{N-1} (i-j)^2 PM \right)$

TC\_9 GLCM Correlation,  $\left( \sum_{i=0}^{N-1} \sum_{j=0}^{N-1} (ij) PM - \mu_x \mu_y \right) / \sqrt{V_x V_y}$

TC13 GLCM Variance,  $V_x$

TC18 Coefficient of Variation,  $\sqrt{V_x V_y} / \mu_x \mu_y$

TC21 Entropy,  $\sum_{i=0}^{N-1} \sum_{j=0}^{N-1} (PM) (-\ln(PM))$

TC23 Difference Entropy,  $\sum_{i=0}^{N-1} P_{x-y}(i) \log_e(P_{x-y}(i))$

TC30 Local Homogeneity,  $\sum_{n=0}^{N-1} (P_{x-y}(n) / (1+n^2))$

TC31 GLCM Mean  $0.5 \cdot (\mu_x + \mu_y)$

| histogram | cube side length in [mm] | TC_1 Angular Second Moment | TC_3 Inverse Different Moment | TC_4 Diagonal Moment | TC_9 Correlation | TC18 Coefficient of Variation | TC21 Entropy | TC30 Local Homogeneity | TC13 Sum of squares / Variance | TC31 Mean    | TC13/TC31 Variance /Mean ratio |
|-----------|--------------------------|----------------------------|-------------------------------|----------------------|------------------|-------------------------------|--------------|------------------------|--------------------------------|--------------|--------------------------------|
| cs        | 2.5                      | 111.9                      | 4.2                           | -27.1                | -15.2            | 22.5                          | -8.4         | 4.2                    | -2.2                           | -10.6        | 9.5                            |
| cs        | 5.0                      | 106.4                      | 7.5                           | -27.3                | -20.0            | 28.9                          | -8.0         | 7.5                    | -16.8                          | -19.6        | 3.5                            |
| cs        | 7.5                      | 85.8                       | 9.0                           | -23.3                | -22.3            | 46.6                          | -6.7         | 9.0                    | -17.7                          | -25.1        | 9.8                            |
| cs        | 10.0                     | 68.6                       | 10.5                          | -20.2                | -19.2            | 77.0                          | -5.6         | 10.5                   | -15.6                          | -30.9        | 22.2                           |
| <b>cs</b> | <b>mean</b>              | <b>93.2</b>                | <b>7.8</b>                    | <b>-24.5</b>         | <b>-19.2</b>     | <b>43.7</b>                   | <b>-7.2</b>  | <b>7.8</b>             | <b>-13.1</b>                   | <b>-21.6</b> | <b>11.3</b>                    |
| hm        | 2.5                      | 111.9                      | 2.3                           | -27.2                | -11.7            | -0.7                          | -8.4         | 2.3                    | -0.4                           | 0.1          | -0.6                           |
| hm        | 5.0                      | 106.4                      | -0.4                          | -24.9                | -15.6            | -0.1                          | -8.0         | -0.4                   | -0.3                           | -0.1         | -0.2                           |
| hm        | 7.5                      | 85.8                       | 0.4                           | -21.5                | -16.1            | -1.0                          | -6.8         | 0.4                    | -1.3                           | -0.2         | -1.1                           |
| hm        | 10.0                     | 68.6                       | 2.1                           | -18.7                | -13.8            | 0.1                           | -5.6         | 2.1                    | -1.1                           | -0.6         | -0.5                           |
| <b>hm</b> | <b>mean</b>              | <b>93.2</b>                | <b>1.1</b>                    | <b>-23.1</b>         | <b>-14.3</b>     | <b>-0.4</b>                   | <b>-7.2</b>  | <b>1.1</b>             | <b>-0.8</b>                    | <b>-0.2</b>  | <b>-0.6</b>                    |

**Table 1:** Sensitivity of textural parameters to a 40% reduction in ventilated lung volume. The latter was achieved by randomly inserting black cubes of side length 2.5, 5, 7.5 and 10mm into the simulated lung. Results are shown as relative changes in the textural parameter for either preparing the data in a histogram-matched (hm) or a contrast-stretched (cs) way and as a mean over 5 distances used in the GLCM calculation.

| Histogram | TC 1<br>Angular<br>Second<br>Moment | TC 3<br>Inverse<br>Different<br>Moment | TC 4<br>Diagonal<br>Moment | TC 9<br>Corre<br>lation | TC18<br>Coefficient<br>of<br>Variation | TC21<br>Entro<br>py | TC30<br>Local<br>Homog<br>eneity | TC13<br>Sum of<br>squares<br>(Variance) | TC31<br>Mean | TC13/<br>TC31<br>Variance<br>/Mean<br>ratio |
|-----------|-------------------------------------|--|----------------------------|-------------------------|--|---------------------|----------------------------------|---|--------------|---|
| cs        | -62.6                               | -2.9                                   | 53.4                       | 10.8                    | -10.8                                  | 11.5                | -2.9                             | 8.7                                     | 10.4         | -1.5  |
| hm        | -62.3                               | -3.9                                   | 48.5                       | 9.0                     | 0.5                                    | 11.3                | -3.9                             | -0.1                                    | -0.3         | 0.2   |

**Table 2:** Sensitivity of textural parameters to a 40% increase in gamma counts. The simulated defects have a cube side length of 10mm. Listed are the differences in the values of the textural parameters derived from either the standard simulation with 40% NVV and associated drop in average brightness and an alternative simulation with a higher gamma count such that after knocking out 40% of the ventilated volume the IOD matched the IOD of the perfectly ventilated lung simulation.

**Figure captions**

**Figure 1:** Illustration of textural parameter TC18, Coefficient of Variation, from the simulation study for cube-shaped defects of size 7.5mm cube side length as a function of non-ventilated lung volume in percent. The GLCMs were created for 5 pixel distances each (1, 2, 4, 8, 12 pixels) corresponding to distances in the lung of 4.7, 9.3, 18.7, 37.3 and 56.0mm, respectively. The coefficient of variation is larger for small pixel distances and increases with NVV and more rapidly so for larger defects (not illustrated).

**Figure 2:** Relative ventilated lung volume (solid black) and standard variation (hashed) per patient group.

**Figure 3:** Illustration of textural parameter TC18, the Coefficient of Variation, for a set of 5 'normal' lungs (left) and a set of 5 lungs of patients suffering from COPD (right). The severity of COPD increases from top to bottom.

**Figure 4:** Textural parameter 18 (solid black) and standard deviation (hashed) from the invariant GLCM and for all 5 distances for the 5 patient groups studied

**Figure 5:** Ratio of textural parameter 30/31 (solid black) and standard deviation (hashed) from the invariant GLCM and mean over 5 distances for the 5 patient groups studied

**Figure 6:** High correlation between ventilated lung volume in percent and textural parameter 18 (coefficient of variation) ( $r^2=0.955$ ).

**Figure 7:** Correlation between textural parameter TC13/TC31 (Variance over Mean ratio) and independent spirometry data (FeV1) for 4 of the 5 patient groups. No spirometry data was available for the 'normal' group. The quality of the linear regression is  $r^2=0.66$ .

FIGURE 1

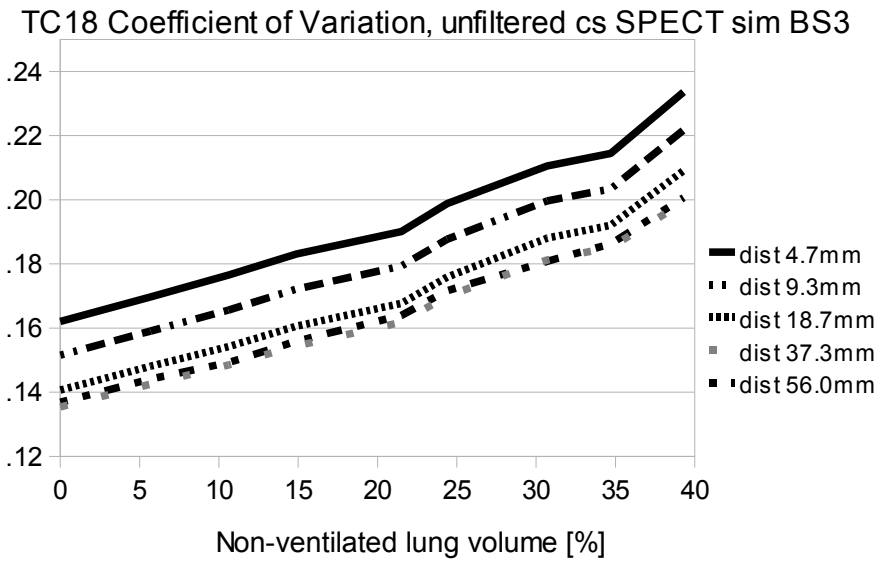


FIGURE 2

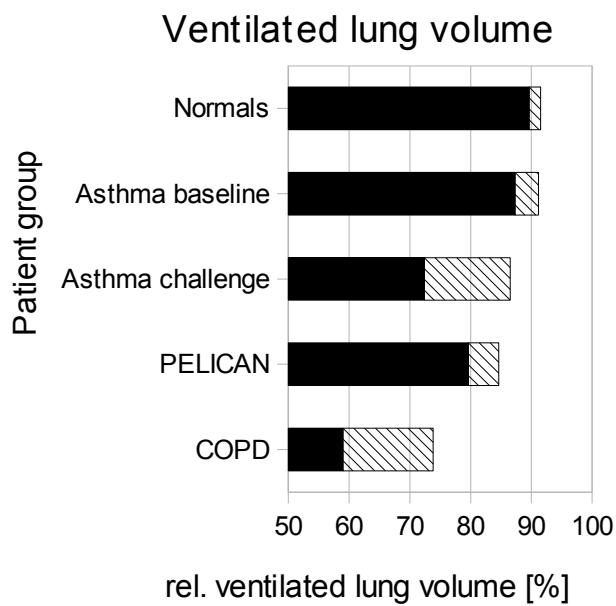


FIGURE 3 (left and right panel, reproduction in black-and-white)

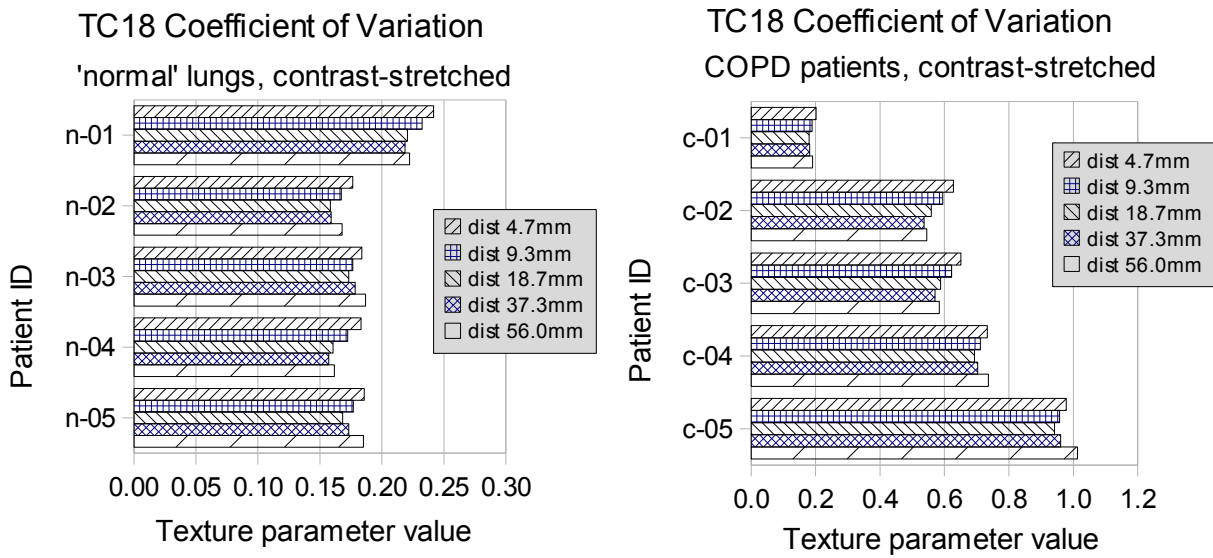


FIGURE 4

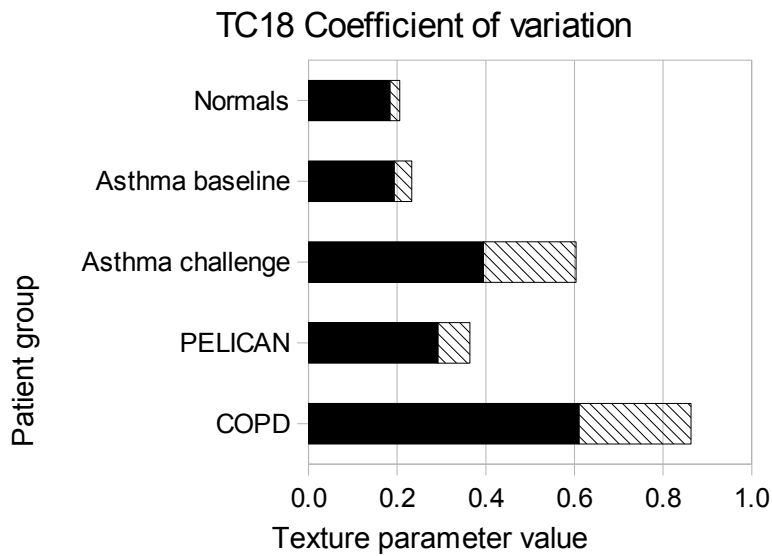




FIGURE 5

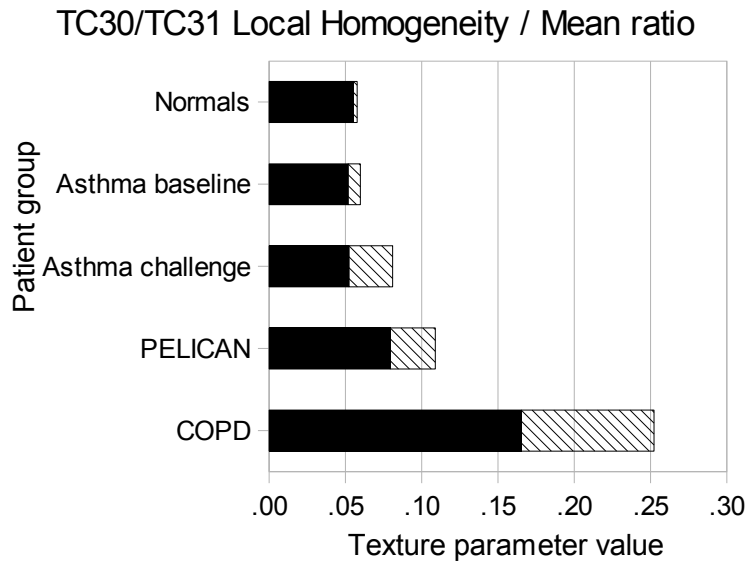


FIGURE 6 (colour reproduction for web-publishing, black-and-white for print)

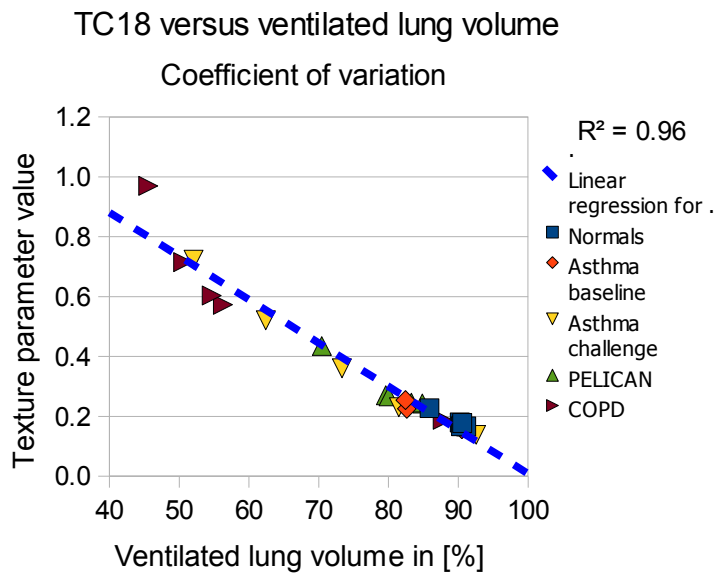
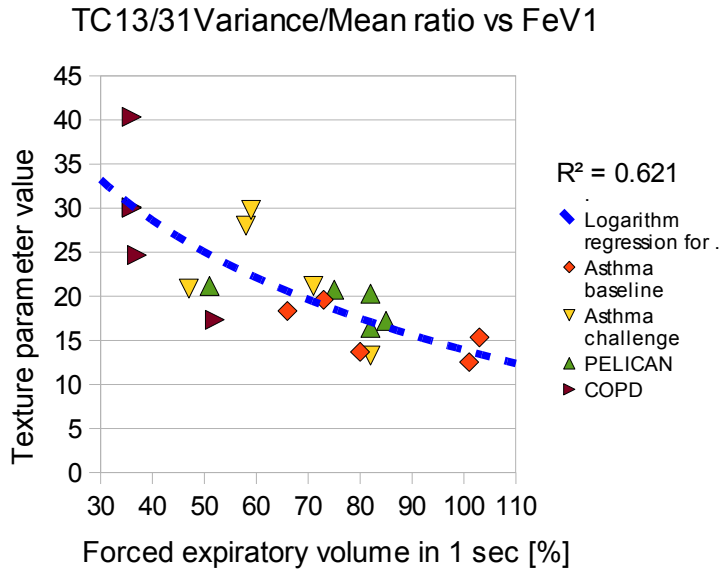


FIGURE 7 (colour reproduction for web-publishing, black-and-white for print)



1  
2  
3  
4  
5  
6  
7  
8  
9  
10  
11  
12  
13  
14  
15  
16  
17  
18  
19  
20  
21  
22  
23  
24  
25  
26  
27  
28  
29  
30  
31  
32  
33  
34  
35  
36  
37  
38  
39  
40  
41  
42  
43  
44  
45  
46  
47  
48  
49  
50  
51  
52  
53  
54  
55  
56  
57  
58  
59  
60  
61  
62  
63  
64  
65

## Application of Texture Analysis to Functional Pulmonary CT Data

Arndt Meier<sup>a</sup>, Catherine Walsh<sup>b,c,d</sup>, Benjamin E. Harris<sup>b,c,d</sup>, Gregory G.King<sup>b,c,d</sup>, and Allan Jones<sup>a</sup>

a) Australian Key Centre for Microscopy and Microanalysis, The University of Sydney, Sydney 2006, NSW, Australia, email: [a.meier@usyd.edu.au](mailto:a.meier@usyd.edu.au) (*corresponding author*)

b) Department of Respiratory Medicine, Royal North Shore Hospital, St Leonards NSW 2065

c) Woolcock Inst. of Medical Research, 431 Glebe Point Road, Glebe, NSW 2037

d) Northern Clinical School, Faculty of Medicine, University of Sydney, Sydney, 2006

1 **Abstract**  
2  
3

4 It is demonstrated that textural parameters calculated from functional pulmonary CT data  
5 have the potential to provide a robust and objective quantitative characterisation of  
6 inhomogeneity in lung function and classification of lung diseases in routine clinical  
7 applications. Clear recommendations are made for optimum data preparation and textural  
8 parameter selection.  
9

10  
11  
12 A new set of platform-independent software tools are presented that are implemented as plug-  
13 ins for ImageJ. The tools allow segmentation and subsequent histogram-based and grey-level  
14 co-occurrence matrix based analysis of the regions of interest. The work-flow is optimised  
15 for use in a clinical environment for the analysis of transverse Computed Tomography (CT)  
16 scans and lung ventilation scans based on SPECT. Consistency tests are made against other  
17 texture analysis plug-ins and simulated lung CT data. The same methods are then applied to  
18 patient data consisting of a healthy reference group and one patient group each who suffered  
19 from asthma, chronic obstructive pulmonary disease (COPD), and COPD plus lung cancer.  
20  
21  
22 The potential for disease classification based on computer analysis is evaluated.  
23  
24  
25  
26  
27  
28  
29  
30  
31  
32  
33  
34  
35  
36  
37  
38  
39  
40  
41  
42  
43  
44  
45  
46  
47  
48

49 **KEYWORDS:**  
50

51  
52 texture analysis, computed tomography, asthma, COPD, lung ventilation  
53  
54  
55  
56  
57  
58  
59  
60  
61  
62  
63  
64  
65

## 1. Introduction

Close to 10 percent of the world population are suffering from chronic lung diseases. The two most common categories, which account for 7.7%, are asthma and chronic obstructive pulmonary disease (COPD).

According to World Health Organisation (WHO) estimates, 300 million people suffer from asthma and 255 000 people died of asthma in 2005 (WHO, 2008a) and an increase of 20% is expected over the next 10 years. Asthma is the most common chronic disease among children.

It is characterised by episodic airway narrowing that occurs on exposure to stimuli, such as exercise, dust, pollens and cold air. Asthmatic lungs are characterised by inhomogeneous ventilation when studied by pulmonary function techniques or by imaging methods. The severity of the inhomogeneity, measured by pulmonary function, is strongly related to the sensitivity of airways to inhalants, i.e. dust, pollens etc. Thus characterisation of the topographical pattern of ventilation in asthmatic lungs is important

The WHO estimates (2007), currently 210 million people suffer from chronic obstructive pulmonary disease (COPD) with 3 million people dying of COPD in 2005 (WHO, 2008b).

COPD is a chronic disease that is caused predominantly by tobacco smoking in western countries. COPD causes lung destruction, known as emphysema, and diseases of small and large airways, which result in cough, mucous production and airway narrowing with resultant breathlessness during exertion.

Single-photon emission computed tomography (SPECT) ventilation scanning (Petersson *et al.*, 2007) using Technetium-99 (Technegas<sup>TM</sup>), is a three dimensional imaging technique used routinely in clinical nuclear medicine for diagnosis of diseases such as pulmonary embolism, when combined with imaging of blood flow (Harris *et al.*, 2007). Ventilation scans, however, have been adapted for studies of ventilation in airways disease (King *et al.*, 1997 and 1998,

1 Downie *et al.*, 2007). SPECT imaging offers the potential to characterise the topographical  
2  
3 distribution of ventilation so that inhomogeneity can be quantified at the regional level (Xu *et*  
4  
5 *al.*, 2001, Venegas *et al.*, 2005). Combining imaging information with the pulmonary function  
6  
7 measures of inhomogeneity will provide important information about the ventilatory  
8  
9 abnormalities in asthma and COPD (Tgavalekos *et al.*, 2007, Berend *et al.*, 2008). However,  
10  
11 suitable methods for quantifying the distribution of ventilation from SPECT data have not  
12  
13 been determined.  
14  
15  
16  
17

18 In this study, we investigate several potentially useful methods of quantifying the distribution  
19  
20 of ventilation from SPECT ventilation data using both simulated SPECT data and data from  
21  
22 well-described clinical groups. The new technique is based on texture analysis and can  
23  
24 provide an objective indicator of abnormal lung conditions.  
25  
26  
27  
28  
29  
30  
31

## 32 **2. Methods**

33  
34

35 We developed new techniques for multiple 3D texture analysis and conventional 3D image  
36  
37 analysis of clinical SPECT data of volumes representing lung tissue as identified from co-  
38  
39 registered CT scans that were obtained at the time of the SPECT.  
40  
41  
42

43 The new technique uses the anatomical CT to define the lung outlines, co-registers these with  
44  
45 the functional SPECT data and performs an image analysis on the voxels of the SPECT thus  
46  
47 defined as representing lung tissue. The image analysis comprises a traditional direct analysis  
48  
49 of the grey levels in the SPECT slices and a texture parameters analysis derived from grey-  
50  
51 level co-occurrence matrices (GLCM) (Haralick, *et al.*, 1973, Choi, 2006).  
52  
53  
54  
55  
56  
57  
58

### 59 **2.1 Simulation data**

60  
61  
62  
63  
64  
65

1 We created a series of SPECT-V data sets based on simulated data to validate the software.

2  
3 The lung phantom used in the construction of the model was based upon X-ray computed  
4 tomography (CT) data from a male of height 178 cm, weighing 70 kg (Zubal *et al.*, 1994) in  
5 supine position, who was chosen for his similarity to the dosimetry standard mathematical  
6 phantom. The Monte Carlo simulation package used for this work was the Photon History  
7 Generator (Lewellen *et al.*, 1988, Haynor *et al.*, 1991), which models the emission, scatter and  
8 attenuation of photons in a heterogeneous phantom, followed by the photons' subsequent  
9 collimation and detection (Chicco *et al.*, 2001).

10  
11 Simulations were performed for a 23.6-mm-thick parallel-hole collimator, using a 32.5-cm  
12 radius of rotation. The isotope modelled was Tc99, collected with a symmetric 20% energy  
13 window centred around 140 keV into a 128×128 matrix with 120 views at equal angular  
14 spacing around 360°, resulting in 5 million counts total when no defects were present. Pixel  
15 resolution was 2.5mm/pixel. To test for any dependence on brightness changes we repeated  
16 two simulations with 9 million counts. These settings were chosen to closely mimic typical  
17 clinical settings when collecting SPECT-V data (similar contrast, spatial resolution and signal  
18 to noise).

19  
20 A series of studies were performed in four groups, distinguished by the size of individual  
21 defects, to simulate the effects of non-ventilated lung tissue. Defects in groups 1–4 were  
22 1x1x1 pixels (15 mm<sup>3</sup>), 2x2x2 pixels (125 mm<sup>3</sup>), 3x3x3 pixels (422 mm<sup>3</sup>) and 4x4x4 pixels  
23 (1000 mm<sup>3</sup>) in size, respectively. These were distributed uniformly throughout both lung  
24 halves in a random manner. Within each group, the amount of lung tissue involved in defects  
25 varied from 0% (normal) up to 40% in steps of 5%, giving 9 studies in each group.

26  
27 These simulated lung data sets were then subjected to normal clinical processing. Lungs  
28 were reconstructed at the same resolution as routine SPECT data (128 slices with 128x128  
29 pixels, voxel size 4.664mm<sup>3</sup>). The lung outlines were known from the original phantom and  
30  
31  
32  
33  
34  
35  
36  
37  
38  
39  
40  
41  
42  
43  
44  
45  
46  
47  
48  
49  
50  
51  
52  
53  
54  
55  
56  
57  
58  
59  
60  
61  
62  
63  
64  
65

1 converted to a binary mask which was then subjected to 2 iterations with the standard ImageJ  
2  
3 erosion operation using a count of 3 (minimum 3 of the nearest neighbour pixels need to be  
4  
5 background pixels for the present pixel to be eroded).  
6  
7  
8  
9  
10

## 11 **2.2 Clinical data**

12  
13  
14  
15 Three groups of patients were studied to evaluate the applicability of the new methods. Five  
16  
17 patients had asthma (data set A), and 10 current or ex-smokers that had either diagnosed  
18  
19 COPD (data set C) or were being evaluated for treatment of lung cancer (PELICAN<sup>1</sup> data set)  
20  
21 who had a wide range of severity of COPD, and scans from 5 patients who underwent lung  
22  
23 scanning for suspected pulmonary embolism but who were considered to have normal lung  
24  
25 scans on routine clinical assessment (data set N).  
26  
27  
28  
29

30 All subjects inhaled Technegas as the ventilation imaging agent. Patients had scans according  
31  
32 to the standard clinical protocol whereby Technegas was inhaled from the Technegas  
33  
34 generator by 1-2 deep inspirations followed by a breath hold to maximise Technegas particle  
35  
36 deposition.  
37  
38  
39

40 Subjects had a ventilation SPECT scan and a CT scan acquired by a dual-detector variable  
41  
42 angle hybrid SPECT/CT system (Phillips SKYLIGHT and Picker PQ5000 CT). All SPECT  
43  
44 studies were acquired using a 128 x 128 matrix, at 15 seconds per stop with 3 degree steps  
45  
46 over 360 degrees. Low-dose CT was performed using non-contrast (30mA, 10kVp, pitch 1.5,  
47  
48 slice thickness 4mm). Study was acquired during tidal breathing. CT images are reconstructed  
49  
50 using a 512 x 512 matrix with a smooth algorithm.  
51  
52  
53  
54

55 Spirometry, including the predicted forced expiratory volume during one second (FeV1), was  
56  
57  
58

---

59  
60 <sup>1</sup> PELICAN study: Predicting Exercise tolerance and Lung function using Imaging in  
61 patients undergoing CANCER Surgery, Royal North Shore Hospital, internal study, 2007.  
62  
63  
64  
65



1 obtained in all groups except the normal group, using standard methods in the lung function  
2  
3 laboratory.  
4  
5  
6  
7  
8

## 9 **2.3 Software**

10 Custom plug-ins were developed for ImageJ (Rasband, 1997-2008) to read and write CT data  
11  
12 routinely stored in Interfile data format (Craddock et al., 1989). Segmentation of the lungs in  
13  
14 the CT datasets is done with a custom written plug-in “Extract\_Lungs”, which was more  
15  
16 efficient than existing segmentation plug-ins (Parker, 2008, Castleman, 2005). Segmentation  
17  
18 uses an edge-following algorithm that stays between an upper and lower grey-value threshold.  
19  
20 If the initial seed-point falls outside the thresholds, a new seed-point is automatically  
21  
22 determined from a search towards the median point of the previous slice and an outward  
23  
24 spiral from there if that fails.  
25  
26  
27  
28  
29  
30

31 Up to 5 regions of interest per slice are supported which are categorised as belonging to either  
32  
33 the left or right lungs. A custom-built ROI manager allows superimposition of the ROIs onto  
34  
35 SPECT ventilation data. The identified volumes are analysed for total area, mean, median,  
36  
37 modal, minimum, and maximum grey values, kurtosis, integrated optical density (IOD), and  
38  
39 histogram. Weighted means are calculated for left, right and total lung.  
40  
41  
42  
43  
44

45 Anatomical CT data were registered to corresponding functional data (SPECT) with the  
46  
47 ImageJ plug-in Align3\_TP (Parker, 2008) with all parameters left to their default values. The  
48  
49 outlines of the registered lung mask were then auto-detected with our segmentation algorithm  
50  
51 resulting in ImageJ standard ROIs (regions of interest). Our modified ROI manager limits all  
52  
53 subsequent analysis to within the defined ROIs.  
54  
55  
56  
57

58 From these ROIs that represent the total lung volume, GLCMs are calculated for the x, y, z,  
59  
60 and invariant orientation for a set of up to 5 chosen distances. These are then subjected to  
61  
62  
63  
64  
65

1 standard texture analysis. We verified the correct implementation of the GLCM algorithm by  
2  
3 comparing results from an independently written plug-in [Cabrera, 2005], which calculates 4  
4  
5 of the 12 textural features we determine, and found both to be consistent.  
6  
7

8  
9 Our methods are based on software that is easily available, widely used, modular in design,  
10  
11 open source and not limited to a specific operating system. ImageJ (Rasband, 1997-2008),  
12  
13 Abramoff *et al.*, 2004, Burger & Burge, 2008) fulfils all these criteria perfectly. And more so,  
14  
15 there is a very large collection of plug-ins publicly available  
16  
17 (<http://rsb.info.nih.gov/ij/plugins/>). The code used in this study is available from the author.  
18  
19  
20  
21  
22  
23

## 24 **2.4 Analysis**

25  
26  
27 In both the simulated and the clinical data the volumes representing lung tissue were  
28  
29 identified as described above. All voxels outside the eroded ROIs were excluded from the  
30  
31 analysis. Note that lung tissue outlines were registered to the reconstructed SPECT data, thus  
32  
33 avoiding any interpolation in the SPECT data set.  
34  
35  
36

37  
38 All SPECT data sets, simulated and clinical, were prepared in two parallel streams: *CS*  
39  
40 (contrast stretched) and *HM* (histogram matched). The contrast stretched data set was created  
41  
42 by first stretching the contrast within the 16-bit grey-levels image stack using the stack  
43  
44 histogram (built-in ImageJ function) and then converting the image stack to an 8-bit grey-  
45  
46 level image stack. The latter step used an improved version of the ImageJ Stack Converter  
47  
48 that uses the stack histogram as opposed to the histogram of the current slice and allows to  
49  
50 fold a set percentage of hot pixels into the highest remaining histogram channel. We chose the  
51  
52 0.02% brightest non-background pixels to be treated as hot pixels.  
53  
54  
55  
56

57  
58 The histogram-matched data set used the histogram from the best ventilated simulated lung as  
59  
60 the reference histogram after smoothing it twice with a Gaussian filter of 5 histogram  
61  
62  
63  
64  
65

1 channels width. This histogram compared well with histograms obtained from patients with  
2  
3 normal lung function. The histogram matcher we wrote uses the stack histogram and can  
4  
5 directly map a 16-bit image stack onto an 8-bit reference histogram thus considerably  
6  
7 reducing channel pile-up effects commonly encountered when first converting from 16-bit to  
8  
9 8-bit and then again from 8-bit to 8-bit reference histogram.

10  
11  
12  
13 The 'extracted lungs' as defined by sets of ROIs were then analysed in two steps. The normal  
14  
15 grey value analysis calculated the total lung volume in voxels, the ventilated volume, the  
16  
17 minimum, mean, modal, median and maximum grey values, IOD, contrast, histogram, and  
18  
19 Kurtosis on a per-ROI basis. Mean values weighted by ROI area were calculated for left,  
20  
21 right, and total lung.  
22  
23  
24

25  
26 A voxel was considered to represent ventilated lung tissue if it had a grey value larger than  
27  
28 20% of the histogram maximum. To minimise the impact of any erratic hot pixels, the  
29  
30 histogram maximum was calculated from the 97% level assuming that the histogram above  
31  
32 97% drops with a slope of -0.5. In this work we only report the results for total lungs, but it is  
33  
34 noted that the software reports more details where this may be of interest.  
35  
36  
37

38  
39 The second step of the analysis created 8-bit grey-level co-occurrence matrices (GLCMs)  
40  
41 from all the ROIs of any one lung for 5 distances each: 1, 2, 4, 8, and 12 pixels (4.7, 9.3, 18.7,  
42  
43 37.3, 56.0mm) and for 4 direction pairs each: X (left->right, right->left), Y (top->bottom,  
44  
45 bottom->top), Z (up->down, down->up) and I (invariant, combining X, Y, and Z). The  
46  
47 invariant matrix we chose gives equal weight to each valid voxel pair and may at times differ  
48  
49 from a mean over the X, Y, and Z matrices as individual matrices may not have the exact  
50  
51 same number of voxel pairs. From these GLCMs twelve texture features were calculated as  
52  
53 listed in appendix A (Haralick *et al.*, 1973, Haralick 1979, Choi, 1996).  
54  
55  
56  
57  
58  
59  
60  
61  
62  
63  
64  
65

### 3. Results

#### 3.1 Results from the phantom study

The texture parameters calculated from the simulated lungs show a number of correlations with the size of the defects and the total non-ventilated volume (NVV). Figure 1 illustrates this for the example of the textural parameter TC18 (coefficient of variation) and simulated defect sizes of 3x3x3 pixels. For all GLCM distances and defect sizes the parameter TC18 increases steadily with increasing NVV and more rapidly so for larger defects.

No significant differences were found between results obtained from X, Y, and Z GLCMs.

Hence only the invariant GLCMs have been studied further. For all 12 textural parameters studied we found under all conditions that the functions such as in Figure 1 are smooth and steady and that different distances in GLCM calculation result in slightly shifted versions of the same shape but that in no case does the graph of one distance cross the graph of another distance for otherwise identical settings. On the contrary, we often saw that graphs for different distances were almost undistinguishable from one another. Consequently the data from all distances were pooled into one; thus reducing the complexity of the results presented. Notwithstanding this, it is noted, that TC9 and TC30 were somewhat more sensitive to NVV changes at shorter distances and that TC2 showed no dependence on NVV but gave significantly different results for different distances.

For clarity only the relative changes in textural parameters between the lowest and highest NVV studied are reported, because the functions change smoothly with NVV and in-between values do not add much to the discussion.

Table 1 lists the relative changes in the textural parameters calculated in response to a 40% drop in ventilated lung volume. Some textural parameters are more sensitive to the changes in ventilated volume than others as can be seen from Table 1 (rows 6 and 11 “*mean*”). Also,

1 they are typically stronger in the contrast-stretched data set (*cs*, row 6) as compared to the  
2  
3 histogram-matched data set (*hm*, row 11).  
4  
5

6 The results from a sensitivity test to brightness changes are shown in Table 2. We repeated the  
7  
8 simulation for the “worst” lung with a higher activity such that after adding the defects it  
9  
10 resulted in the same IOD as the perfectly ventilated simulated lung. Insensitivity to brightness  
11  
12 changes would allow the direct comparison of textural parameters derived from studies that  
13  
14 use different gamma counts. Note that rows 2 and 3 in Table 2 correspond to rows 5 and 10 in  
15  
16 Table 1 (10 mm), respectively, but the percentage changes are expressed relative to the values  
17  
18 in Table 1. It is noted that the sign of all values in Table 2 act in such a way as to reduce the  
19  
20 sensitivity of the textural parameters.  
21  
22  
23  
24  
25

26 In the context of our work a good textural parameter is one that is sensitive to changes in  
27  
28 NVV or defect-size and that is at the same time insensitive to changes in brightness. With this  
29  
30 in mind we can group the textural parameters investigated into robust, intermediate and poor  
31  
32 performers:  
33  
34  
35  
36  
37  
38  
39

#### 40 **Robust textural parameters:**

41  
42 TC13/TC31 Variance/Mean ratio: provides a solid signal of 22% change in the parameter  
43  
44 value for a 40% change in NVV while its dependence on brightness doubling is only small  
45  
46 (1.5%). The sensitivity is somewhat poorer for smaller defects.  
47  
48  
49

50 TC30 Local homogeneity: provides still a good signal of 10.5% change for a 40% drop in  
51  
52 NVV but is more sensitive to brightness changes than the TC13/TC31 ratio (2.9%).  
53  
54  
55

56 TC18 Coefficient of Variation: provides a very strong signal of 77% for large defects and a  
57  
58 still strong signal of 22% for small defects. It has a moderate dependence on brightness  
59  
60 changes (10.8% simulating large defects). However, correlation with clinical data discussed  
61  
62  
63  
64  
65

1 below is excellent.  
2  
3  
4  
5  
6

7 **Textural parameters with intermediate performance:**  
8

9  
10 TC1 Angular second moment: provides high sensitivity (>68%) to changes in NVV, but  
11  
12 unfortunately it is also very sensitive to brightness changes.  
13  
14

15 TC2 and TC2: Difference and inverse difference moment: show a modest sensitivity for short  
16  
17 distances and small-sized defects but are insensitive at larger pixel distances as well as for  
18  
19 larger defect sizes. However, they may be used successfully in conjunction with other  
20  
21 parameters to decide whether the effective size distribution of the non-ventilated volumes is  
22  
23 small or large.  
24  
25  
26

27  
28 TC9 Correlation: The theoretical study shows a reasonable sensitivity of around 20% to  
29  
30 changes twice that large in NVV but also a relatively high sensitivity to brightness changes. In  
31  
32 the clinical studies discussed below this parameter did not convince and is outperformed by  
33  
34 others.  
35  
36  
37  
38  
39  
40

41 **Textural parameters with poor performance:**  
42

43  
44 TC7, TC4, TC13, TC31, TC21, and TC23: These parameters suffer either from a lack of  
45  
46 sensitivity or high sensitivity to changes in brightness.  
47  
48  
49  
50  
51

52 **Combination of textural parameters:**  
53

54  
55 The ratio of TC13/TC31 is a very good performer although neither TC13 nor TC31 are good  
56  
57 performers. Similarly, the ratio of TC21/TC31 gives a moderately good performance.  
58  
59  
60  
61  
62  
63  
64  
65

### 3.2 Results from the clinical studies

Figure 2 illustrates the estimated ventilated lung volume grouped by patient group. The 'normal' group shows the highest ventilated volume of about 90% and the smallest variance. Asthmatic lungs at baseline show a slightly lower ventilated lung volume although not statistically significant from the 'normal' lungs. The remaining patient groups show significant reductions in ventilated lung volume that are strongest in COPD patients. There is also a higher variability in these groups.

Figures 3 and 4 illustrate one of the best performing textural parameters for the 5 patient groups studied. Both the absolute value and the variability between different GLCM distances and between patients in the 'normal' lung function group are small (Figure 3, left panel). The results from COPD patients which range from a mild case (right panel, c-01) to severe (c-05) show increasingly higher values.

The differences between using different distances in the GLCM calculations are almost within the numerical precision, which was also observed in the results from the simulated data. This observation holds true for all textural parameters and patient groups studied except for TC2, TC9 and TC30. TC9 (Correlation) and TC30 (Local Homogeneity) lose sensitivity with increasing distance between voxel pairs and better performance is achieved by only using the 2 shortest distances (1 and 2 pixels distance corresponding to 4.7 and 9.3mm, respectively). TC2 will be discussed separately below. These findings are consistent with observations from the simulated data.

Pooling the data from all GLCM distances<sup>2</sup> and by patient group allows us to look for disease-specific differences as shown in Figure 4. While asthmatics at baseline cannot be distinguished from normal lungs, they can be clearly identified after a Metacholine challenge. PELICAN patients and even more so COPD patients have strongly elevated values in the coefficient of

---

<sup>2</sup> Except for TC9 and TC30 which pooled only the 2 shortest distances for higher sensitivity

1 variation calculated from the GLCM.

2  
3  
4 Figure 5 presents the ratio of Local Homogeneity and GLCM Mean (TC30/TC31) calculated  
5  
6 in the same way as in the previous figure. Again, values for COPD and PELICAN patients are  
7  
8 significantly higher than those for normal and asthmatic lungs. It is noted, however, that  
9  
10 asthma patients both at baseline and at Metacholine challenge give almost identical results.  
11  
12 Hence combining the information from multiple textural parameters allows to distinguish  
13  
14 between different disease classes such as asthma from COPD.  
15  
16

17  
18  
19 A very strong correlation ( $r^2=0.955$ ) between the textural parameter Coefficient of Variation  
20  
21 (TC18) and the estimated ventilated lung volume is illustrated in Figure 6. Similarly high  
22  
23 correlations of  $r^2>0.8$  exist for textural parameters TC3, TC30, TC31, and the ratios  
24  
25 TC13/TC31 and TC21/TC31 as a function of ventilated lung volume (not illustrated). More  
26  
27 positive correlations ( $r^2>0.49$ ) are observed for textural parameters TC1, TC9, and the ratio  
28  
29 TC1/TC31.  
30  
31

32  
33  
34 Independent spirometry data in the form of the predicted forced expiratory volume during 1  
35  
36 second (FeV1) was available for all but the 'normal' group. Again good correlations are  
37  
38 observed with several textural parameters ( $r^2>0.5$  for TC18 and TC13/TC31,  $r^2>0.4$  for TC3,  
39  
40 TC30, TC21/TC31, TC31 and TC1/TC31 and  $r^2>0.3$  for TC1, TC2 and TC9) as illustrated in  
41  
42 Figure 7 for the example of TC13/TC31.  
43  
44

45  
46 The Difference Moment (TC2) behaves differently from all other textural parameters studied.  
47  
48 It is insensitive to changes in both NVV and FeV1, but it is sensitive to the size distribution of  
49  
50 patterns in the lung. Hence the TC2 textural parameter results were prepared in a different  
51  
52 way. Instead of pooling the results from different GLCM distances, the parameter value  
53  
54 obtained with the shortest distance (1 pixel) were divided by the parameter value for the  
55  
56 second largest distance for any one lung and that we refer to as TC2<sub>d</sub> for short. Data prepared  
57  
58 in this way resulted in a positive correlation of TC2<sub>d</sub> with NVV ( $r^2=0.69$ ) and a somewhat  
59  
60  
61  
62  
63  
64  
65



1 weaker correlation with FeV1 ( $r^2=0.375$ ).  
2  
3

4 All results in this section were derived from the contrast-stretched data set as it showed an  
5 overall better performance than compared to results derived from the histogram-matched data.  
6  
7

8 It is noted that TC18, TC31 (Mean) and TC13/TC31 were indifferent to both NVV and FeV1  
9 changes in the histogram-matched data set, but otherwise the same textural parameters  
10 performed well as in the contrast-stretched data set. The only textural parameter that faired  
11 significantly better in the histogram-matched data set was TC23 (Difference Entropy).  
12  
13  
14  
15  
16  
17  
18  
19  
20  
21

## 22 **4 Discussion**

23  
24

25 Changes in the grey level distribution such as a shift to darker grey values – as can be  
26 expected with a reduction in ventilated lung volume – is essentially removed in the histogram-  
27 matched data. Hence, changes in the textural parameters that occur in the contrast-stretched  
28 data set but not in the histogram-matched one are thought to be driven by histogram changes  
29 while changes that occur in the histogram-matched data set are thought to be dominated by  
30 changes in pattern (Table 1). Changes in the contrast-stretched data set are often a result of  
31 both histogram and pattern changes.  
32  
33  
34  
35  
36  
37  
38  
39  
40  
41

42 In an ideal system a change in brightness should not affect the textural parameters calculated  
43 because the GLCMs are always normalised to an IOD of unity. However, it is noted that the  
44 spatial resolution of the observation system is significantly lower than the features that cause  
45 them. The effective resolution in the SPECT-V data is lower than the pixel resolution of  
46 4.664mm/pxl which in turn is much coarser than the simulated small defects starting from  
47 2.5mm cube side length. Due to the nature of discrete sampling – and in this case significant  
48 under-sampling – of the object space and the non-linearity of the resulting effective blurring,  
49 the texture parameters calculated become dependent on the total optical density and contrast  
50  
51  
52  
53  
54  
55  
56  
57  
58  
59  
60  
61  
62  
63  
64  
65

1 in the SPECT-V data sets. This effect itself is also dependent on the effective size distribution  
2  
3 of the defects we seek to describe. To quantitatively describe the exact relationship is  
4  
5 mathematically complex and of limited practical use as it will vary from situation to situation.  
6  
7 Instead we seek to identify textural parameters that depend acceptably little on the variability  
8  
9 in patient data preparation.  
10  
11

12  
13 The simulated data allows to fully control the environment, to know the true size distribution  
14  
15 of the non-ventilated lung volumes, the true ventilated volume, and to vary some of these  
16  
17 parameters systematically to study its impact. However, there are also some differences and  
18  
19 limitations compared to clinical data that are undesirable. One is that the IOD of the simulated  
20  
21 SPECT-V scan drops progressively with increasing NVV due to the simplicity of the model  
22  
23 available to us.  
24  
25

26  
27 A patient with a smaller ventilated lung volume inhales approximately the same amount of  
28  
29 radioactivity as a patient with a larger ventilated lung volume. As a result the scan from the  
30  
31 former patient would have a larger information content<sup>3</sup> and image contrast; because the same  
32  
33 amount of activity has to squeeze into a smaller volume, a wider range of different brightness  
34  
35 values is observed. Hence a poorly ventilated *simulated* lung has a somewhat *lower*  
36  
37 information content in the simulated data in contrast to a patient with a poorly ventilated lung  
38  
39 that would result in a *higher* information content than the ideally ventilated lung. We studied  
40  
41 this behaviour by simulating one data set with a higher gamma count, which resulted in an  
42  
43 increase of 38% in information content as opposed to a 9% drop in the non-corrected  
44  
45 simulation case. Although the textural parameters are modified as a result, it does not change  
46  
47 the overall response to NVV and we were able to identify textural parameters that are little or  
48  
49 non-susceptible to this change (Table 2). This finding is also directly relevant to clinical data,  
50  
51 because any two patients with naturally differently-sized lungs that are administered the same  
52  
53  
54  
55  
56  
57  
58  
59

---

60 <sup>3</sup> We use the term information content in the strict sense of the number of grey values in an associated  
61 histogram that are non-zero.  
62  
63  
64  
65

1 amount of Technegas will have differences in contrast and information content of the SPECT  
2 recorded. Selecting textural parameters that are insensitive to this variability in data collection  
3 is an advantage in data interpretation.  
4  
5

6 Reconstructed SPECT data is routinely subjected to a rather strong smoothing filter before  
7 being presented to a radiographer or other medical professional. Filtering at the RNSH  
8 consists of a 9<sup>th</sup> order Butterworth filter with a cut-off of 1.2 cycles per centimetre. Since  
9 texture analysis by definition looks at small differences in grey values between pairs of pixels,  
10 any smoothing operation degrades the capabilities of the method for any given case. We tested  
11 this expected behaviour by preparing both simulated and normal patient data with and  
12 without applying the Butterworth filter and found the smoothed data set to have a poorer  
13 sensitivity as manifested in smaller relative changes in textural parameters. We will report the  
14 exact impact in a forthcoming separate study. In this work we only discuss reconstructed,  
15 extracted lung data that has **not** been subjected to any post-filtering.  
16  
17  
18  
19  
20  
21  
22  
23  
24  
25  
26  
27  
28  
29  
30  
31  
32

33 A change of distance in the calculation of the GLCMs (within reason) adds little new  
34 information (Figure 1) with the exception of parameter TC2. In most cases the calculation of  
35 the GLCM for only one distance seems to be sufficient. For 2 of the textural parameters  
36 studied there is a better performance seen for shorter distances in the GLCM calculations  
37 (TC9 and TC30). This is plausible looking at the definitions (Appendix 1). Voxel pairs that are  
38 far from one another are unlikely to be highly correlated thus giving low correlation values in  
39 any lung (TC9) and uniformity between them will be near the random value (TC30).  
40  
41  
42  
43  
44  
45  
46  
47  
48  
49  
50

51 From the simulated data it is known that TC2<sub>d</sub> drops with increasing defect size and in the  
52 patient data it drops with increasing NVV. This suggests that the average size of individual,  
53 non-ventilated areas increases with the severity of the diseases studied as opposed to a mere  
54 increase of number of non-ventilated areas of same size. This result is consistent with the  
55 perception of the SPECT data to the human eye.  
56  
57  
58  
59  
60  
61  
62  
63  
64  
65

1 Several well performing textural parameters were identified that by themselves allow to  
2  
3 distinguish between a 'normal' lung and a lung that suffers from some significant medical  
4  
5 condition or disease. Combinations of textural parameters have the potential to further  
6  
7 classify abnormal lungs. For example, to distinguish between asthmatics on one hand and  
8  
9 COPD patients on the other hand one can combine the results from TC18 and the ratio  
10  
11 TC30/TC31. TC18 is elevated in all diseases, but the ratio TC30/TC31 does not rise  
12  
13 significantly in asthmatics while it does rise significantly in COPD patients (compare Figures  
14  
15 4 and 5).  
16  
17  
18  
19  
20

21 Correlation of several key textural parameters with the corresponding ventilated lung volume  
22  
23 are good to excellent for all patient data (Figures 6 and 7). Note that the ventilated lung  
24  
25 volume is a measure that is calculated from the original imaging data (not the GLCM), while  
26  
27 the FeV1 is a completely independent measurement. The pooling of data per disease group  
28  
29 (Figures 4 and 5) combines all patients of one disease into one - independent of the severity of  
30  
31 disease. Figures 6 and 7 on the other hand illustrate the relationship between reduced lung  
32  
33 functionality and resulting changes in derived textural parameters. It is pointed out that  
34  
35 reduced lung functionality goes along with higher heterogeneity in the SPECT data (Berend *et*  
36  
37 *al.*, 2008) and textural parameters that measure heterogeneity increase while parameters that  
38  
39 measure uniformity drop.  
40  
41  
42  
43  
44

45 The textural parameters discussed are not all linearly independent of one another but some of  
46  
47 them have substantial correlations amongst them. (Clausi, 2008). For practical matters it is  
48  
49 desirable to identify a small number of textural parameters that give the overall best  
50  
51 classification performance.  
52  
53  
54  
55

56 TC2, TC3, TC4 and TC30 are all measures of contrast, though with different weights. TC3  
57  
58 and TC30, which weigh values by the inverse of the contrast (homogeneity), have both shown  
59  
60 consistently better performance in all patient data and either one of these two parameters are  
61  
62  
63  
64  
65

1 recommend for use. As TC3 and TC30 are highly correlated one should choose only one of  
2  
3 them with TC3 performing marginally better in contrast-stretched data sets and TC30 better in  
4  
5 histogram-matched data sets.  
6

7  
8 TC1, TC21 and TC23 are all measures of orderliness. The ratio TC21/TC31 performed best in  
9  
10 the clinical data. The GLCM Mean (TC31) reflects brightness changes between patients that  
11  
12 the contrast-stretched data set is susceptible to. Thus using textural parameter combinations  
13  
14 that involve the GLCM Mean improves correlation in several textural parameters studied. The  
15  
16 histogram-matched data set shows no correlation with TC31 and combining textural  
17  
18 parameters with TC31 carries no advantage and TC23 by itself gives the best performance in  
19  
20 the group of textural parameters that measure orderliness. The value of Entropy (TC21, TC23)  
21  
22 increases with increasing heterogeneity.  
23  
24  
25  
26

27  
28 TC9 (Correlation), TC13 (Variance), TC18 (Coefficient of Variation) and TC31 (Mean) are  
29  
30 descriptive statistics of the GLCMs and the frequency at which certain voxel *pairs* occur. The  
31  
32 combination of Variance and Mean in the Coefficient of Variation (TC18) and the Variance  
33  
34 over Mean ratio (TC13/TC31) gave excellent performance in the contrast-stretched data set  
35  
36 and is another recommended parameter for use. TC18 and the TC13/TC31 ratio are highly  
37  
38 correlated parameters. TC18 shows better correlation with ventilated lung volume and  
39  
40 TC13/TC31 shows better correlation with FeV1 but either one being a very good choice for  
41  
42 characterising the clinical data.  
43  
44  
45  
46

47  
48 GLCM Correlation (TC9) Is largely independent of the other texture measures and has the  
49  
50 potential for giving additional insight. TC9 can be calculated for increasingly larger voxel  
51  
52 distances and the size at which the value suddenly decreases is a measure for the size of  
53  
54 definable objects in the original image data. However, we could not identify any 'sharp' drops  
55  
56 but only gradual changes with the clinical data, suggesting that there is a broad size  
57  
58 distribution of objects which makes this approach less powerful. Simply comparing the  
59  
60  
61  
62  
63  
64  
65

1 differences in Correlation values between the shortest and longest distance studied with  
2 ventilated lung volume resulted in a modest correlation ( $r^2=0.41$ ).  
3  
4

5  
6 It is noted that the best correlations between textural parameters and ventilated lung volume  
7 were achieved with a linear regression while correlation with FeV1 gave consistently better  
8 results using a logarithmic correlation function.  
9

10 Summed up the following 3 recommendations can be made for the analysis of pulmonary  
11 SPECT-V data.  
12  
13

- 14 1) Texture analysis sensitivity is maximised by preparing SPECT data in an unfiltered,  
15 contrast-stretched way, as opposed to filtered or histogram-matched.  
16  
17
- 18 2) The choice of voxel pair distance in the GLCM calculation is non-critical. With  
19 present spatial resolution in SPECT data 1, 2, or 3 pixel distances are good choices  
20 that can also be pooled to improve statistics.  
21  
22
- 23 3) Amongst the many textural parameters studied one each should be chosen from 3  
24 different groups of parameters to balance the capability to characterise with the  
25 computational effort involved. These are the textural parameters TC18 or the ratio  
26 TC13/TC31 from the descriptive statistics group, the parameter TC3 or TC30 from the  
27 contrast group and the parameter ratio TC21/TC31 in the orderliness group.  
28  
29  
30  
31  
32  
33  
34  
35  
36  
37  
38  
39  
40  
41  
42  
43  
44

45 Application of the new software package is not limited to pulmonary studies – in fact it may  
46 also be applied to other organs or to completely different fields such as material sciences or  
47 mineralogy. However, in its present form the software package is optimized to the work-flow  
48 of studying lungs in a clinical scenario.  
49  
50  
51  
52  
53

## 54 55 56 57 58 59 **Summary** 60 61 62 63 64 65

1 It has been demonstrated that a textural parameter analysis of functional pulmonary CT data  
2  
3 has the potential to provide a robust and objective quantitative characterisation of  
4  
5 inhomogeneity in lung function and classification of lung diseases with application in routine  
6  
7 clinical applications and national screening programmes. The new methods applied to SPECT  
8  
9 lung ventilation scans are capable of distinguishing between different types of diseases.  
10  
11 Strong correlations between key textural parameters and independent lung function data such  
12  
13 as the FeV1 suggest that a quantitative description of the severity of diseases such as asthma  
14  
15 or COPD by means of derived texture parameters is viable. Clear recommendations have been  
16  
17 made for optimum data preparation and textural parameter selection. In a forthcoming study  
18  
19 we plan to use data from larger numbers of patients and additional spirometry data to further  
20  
21 refine the methods.  
22  
23  
24  
25  
26  
27  
28  
29  
30

### 31 **Acknowledgements**

32  
33 This work is supported by the Australian Research Council through the ARC Linkage Project  
34  
35 LP0562715. The authors are grateful for scientific and technical input and support from the  
36  
37 Australian Microscopy & Microanalysis Research Facility (AMMRF) node at  
38  
39 the University of Sydney. We also like to thank the staff at the Royal North Shore Hospital  
40  
41 that helped in the data collection and the volunteer patients that participated in this study. In  
42  
43 particular we like to thank Peter Chicco, Department of Biomedical Engineering, who  
44  
45 provided the lung simulations, Dale and Elizabeth Bailey, Department of Nuclear Medicine,  
46  
47 for discussion and data conversion.  
48  
49  
50  
51  
52  
53

54 We like to thank Wayne Rasband and all other developers that made contributions to ImageJ  
55  
56 and its plug-ins for sharing their work freely with other researchers (Rasband, 1997-2008,  
57  
58 Abramoff *et al.*, 2004) – without them our work would have been much harder. Part of the  
59  
60  
61  
62  
63  
64  
65

software presented here started their development based on other publicly available plug-ins that are accessible through the ImageJ web page (Rasband,1997-2008, Castleman, 2005, Miller, 2002).

## References

- Abramoff, MD, Magelhaes, PJ, Ram, SJ, Image Processing with ImageJ, Biophotonics International (2004), **11**(7):36-42
- Berend N, Salome CM, King GG, Mechanisms of airway hyper-responsiveness in asthma. *Respirology* (2008), **13**(5):624-631
- Burger W and Burge MJ, Digital Image Processing - An Algorithmic Approach using Java. Springer-Verlag, New York (2008). ISBN 978-1-84628-379-6, [www.imagingbook.com](http://www.imagingbook.com)
- Cabrera JE, “GLCM\_Texture” plug-in for ImageJ, (2005), <http://rsb.info.nih.gov/ij/plugins/>
- Castleman M, “Cell\_outliner” plug-in for ImageJ ([m@mlcastle.net](mailto:m@mlcastle.net)), Columbia University (2005) <http://rsb.info.nih.gov/ij/plugins/cell-outliner.html>
- Chicco P, Magnussen JS, Mackey DW, Bush V, Emmett L, Storey G, Bautovich G, and Wall H van der, SPET of a computerised model of diffuse lung disease, *Eur.J.Nuc.Med* (2001), **28**(2):150-154
- Choi HK, New Methods for Image Analysis of Tissue Sections. PhD thesis, Uppsala University, Sweden (1996), ISBN 91-554-3829-6
- Clausi DA, An analysis of co-occurrence texture statistics as a function of grey level quantization. *Can. J. Remote Sensing*, (2002), **28**(1):45–62
- Craddock TD, Bailey DL, Hutton BF, Conninck F De, Busemann-Sokole E, Bergmann H, and Noelpp U, A standard protocol for the exchange of nuclear medicine image files. *NucMedComm* (1989), **10**:703-713
- Downie SR, Salome CM, Verbanck S, Thompson BR, Berend N and King GG, Ventilation heterogeneity is a major determinant of airway hyperresponsiveness in asthma, independent of airway inflammation. *Thorax* (2007), **62**:684-689
- Haralick RM, Shanmugam K, and Dinstein I, Textural features for image classification. *IEEE Transactions on Systems, Man, and Cybernetics* (1973), **SMC-3**(6):610-621
- Haralick RM, Statistical and structural approaches to texture. *Proceedings of the IEEE* 67 (1979), **5**:786-804
- Harris BE, Bailey D, Miles S, Bailey E, Rogers K, Roach P, Thomas P, Hensley M, and King GG, “Objective analysis of tomographic ventilation perfusion scintigraphy in pulmonary embolism”, *Am. J. Respir. Crit. Care Med.* , March 15, 2007
- Haynor DR, Harrison RL, Lewellen TK, The use of importance sampling techniques to improve the efficiency of photon tracking in emission tomography simulations. *Med Phys* (1991), **18**:990–1001
- King GG, Eberl S, Salome CM, Meikle SR, and Woolcock AJ, Airway closure measured by a Technegas bolus and SPECT. *Am.J.Respir.Crit.CareMed.* (1997) **155**:682–688



- 1 King GG, Eberl S, Salome CM, Young IH, and Woolcock AJ, Differences in airway closure  
 2 between normal and asthmatic subjects measured with single-photon emission computed  
 3 tomography and technegas. *Am.J.Respir.Crit.CareMed.* (1998), **158**:1900–1906.  
 4
- 5 Lewellen TK, Anson CP, Haynor DR, Design of a simulation system for emission  
 6 tomographs. *J Nucl Med* (1988), **29**:871  
 7
- 8 Miller M, “Segmenting\_Assistant”, plug-in for ImageJ, (2002) mmiller3@iupui.edu,  
 9 <http://rsb.info.nih.gov/ij/plugins/index.html>  
 10
- 11 Parker JA, Align3\_TP: stack alignment plug-in for ImageJ, J.A.Parker@IEEE.org (version  
 12 25/Mar/2008), <http://www.med.harvard.edu/JPNM/ij/plugins/Align3TP.html>  
 13
- 14 Petersson J, Sánchez-Crespo A, Larsson SA and Mure M, Physiological imaging of the lung:  
 15 single-photon-emission computed tomography (SPECT). *J Appl Physiol* (2007) **102**:468-476  
 16
- 17 Rasband, W.S., ImageJ, U. S. National Institutes of Health, Bethesda, Maryland, USA,  
 18 <http://rsb.info.nih.gov/ij/>, 1997-2008.  
 19
- 20 Tgavalekos NT, Musch G, Harris RS, Vidal Melo MF, Winkler T, Schroeder T, Callahan R,  
 21 Lutchen KR and Venegas JG, Relationship between airway narrowing, patchy ventilation and  
 22 lung mechanics. *Eur Respir J* (2007), **29**:1174–1181  
 23
- 24 Venegas JG, Schroeder T, Harris S, Winkler RT, and Vidal Melo MF, The distribution of  
 25 ventilation during bronchoconstriction is patchy and bimodal: A PET imaging study.  
 26 *Respiratory Physiology & Neurobiology* (2005) **148**:57–64  
 27
- 28 WHO World Health Organisation, 2008a, <http://www.who.int/respiratory/asthma/en/>  
 29
- 30 WHO World Health Organisation, 2008b, <http://www.who.int/respiratory/copd/en/>  
 31
- 32 Xu J, Moonen M, Johansson Å, Gustafsson A, and Bake B, Quantitative analysis of  
 33 inhomogeneity in ventilation SPET. *Eur J Nucl Med* (2001) **28**:1795–1800  
 34
- 35 Zubal IG, Harrell CR, Smith EO, Rattner Z, Gindi G, Hoffer PB, Computerized three-  
 36 dimensional segmented human anatomy. *Med Phys* (1994), **21**:299–302  
 37  
 38  
 39  
 40  
 41  
 42  
 43  
 44  
 45  
 46  
 47  
 48  
 49  
 50  
 51  
 52  
 53  
 54  
 55  
 56  
 57  
 58  
 59  
 60  
 61  
 62  
 63  
 64  
 65

## Appendix A: Definition of textural features from the co-occurrence matrix

A co-occurrence matrix  $P(i,j|d,\theta)$  (PM for short) contains the probability that the grey level  $i$  occurs at a distance  $d$  in direction  $\theta$  from a pixel with grey value  $j$ .  $N$  is the size of the co-occurrence matrix ( $N=256$  in this study). Integrated sums are calculated from the matrix variance. We further define the vertical ( $p_x(i)$ ), horizontal ( $p_y(i)$ ), minor diagonal ( $p_{x-y}(k)$ ) sums, the vertical ( $\mu_x$ ) and horizontal ( $\mu_y$ ) mean, and the variance of the vertical ( $V_x$ ) and horizontal ( $V_y$ ) directions (Choi, 1996). Note that the GLCM mean is distinct from the mean grey value of the original image because it is weighted by the frequency of occurrence *in combination with* a certain neighbour pixel value.

$$P_x[i] = \sum_{j=0}^{N-1} PM_{ij}, \quad P_y[j] = \sum_{i=0}^{N-1} PM_{ij}, \quad P_{x-y}[k] = \sum_{i=0, i+j=k}^{N-1} \sum_{j=0}^{N-1} PM_{ij}, \quad \mu_x = \sum_i i P_x[i],$$

$$\mu_y = \sum_j j P_y[j], \quad V_x = \sum_i [i - \mu_x]^2 P_x[i], \quad V_y = \sum_j [j - \mu_y]^2 P_y[j]$$

TC\_1 Angular Second Moment  $\sum_{i=0}^{N-1} \sum_{j=0}^{N-1} PM^2$

TC\_2 Difference Moment or GLCM Contrast  $\sum_{i=0}^{N-1} \sum_{j=0}^{N-1} |i-j|^2 PM$

TC\_3 Inverse Difference Moment,  $\sum_{i=0}^{N-1} \sum_{j=0}^{N-1} \frac{1}{|i-j|^2} PM$

TC\_4 Diagonal Moment,  $\sum_{i=0}^{N-1} \sum_{j=0}^{N-1} \frac{1}{|0.5(i-j)|} PM$

TC\_7 Inertia,  $\sum_{n=0}^{N-1} n^2 \sum_{i=0, i-j=n}^{N-1} \sum_{j=0}^{N-1} |i-j|^2 PM$

TC\_9 GLCM Correlation,  $\frac{\sum_{i=0}^{N-1} \sum_{j=0}^{N-1} ij PM - \mu_x \mu_y}{\sqrt{V_x V_y}}$

TC13 GLCM Variance,  $V_x$

TC18 Coefficient of Variation,  $\frac{\sqrt{V_x V_y}}{\mu_x \mu_y}$

TC21 Entropy,  $\sum_{i=0}^{N-1} \sum_{j=0}^{N-1} PM \ln PM$

TC23 Difference Entropy,  $\sum_{i=0}^{N-1} P_{x-y}[i] \log_e P_{x-y}[i]$

TC30 Local Homogeneity,  $\sum_{n=0}^{N-1} \frac{1}{|n|+1+n^2}$

TC31 GLCM Mean  $0.5(\mu_x + \mu_y)$

| histogram | cube side length [mm] | TC_1<br>Angular Second Moment | TC_3<br>Inverse Different Moment | TC_4<br>Diagonal Moment | TC_9<br>Correlation | TC18<br>Coefficient of Variation | TC21<br>Entropy | TC30<br>Local Homogeneity | TC13<br>Sum of squares / Variance | TC31<br>Mean | TC13/TC31<br>Variance / Mean ratio |
|-----------|-----------------------|-------------------------------|----------------------------------|-------------------------|---------------------|----------------------------------|-----------------|---------------------------|-----------------------------------|--------------|------------------------------------|
| cs        | 2.5                   | 111.9                         | 4.2                              | -27.1                   | -15.2               | 22.5                             | -8.4            | 4.2                       | -2.2                              | -10.6        | 9.5                                |
| cs        | 5.0                   | 106.4                         | 7.5                              | -27.3                   | -20.0               | 28.9                             | -8.0            | 7.5                       | -16.8                             | -19.6        | 3.5                                |
| cs        | 7.5                   | 85.8                          | 9.0                              | -23.3                   | -22.3               | 46.6                             | -6.7            | 9.0                       | -17.7                             | -25.1        | 9.8                                |
| cs        | 10.0                  | 68.6                          | 10.5                             | -20.2                   | -19.2               | 77.0                             | -5.6            | 10.5                      | -15.6                             | -30.9        | 22.2                               |
| <b>cs</b> | <b>mean</b>           | <b>93.2</b>                   | <b>7.8</b>                       | <b>-24.5</b>            | <b>-19.2</b>        | <b>43.7</b>                      | <b>-7.2</b>     | <b>7.8</b>                | <b>-13.1</b>                      | <b>-21.6</b> | <b>11.3</b>                        |
| hm        | 2.5                   | 111.9                         | 2.3                              | -27.2                   | -11.7               | -0.7                             | -8.4            | 2.3                       | -0.4                              | 0.1          | -0.6                               |
| hm        | 5.0                   | 106.4                         | -0.4                             | -24.9                   | -15.6               | -0.1                             | -8.0            | -0.4                      | -0.3                              | -0.1         | -0.2                               |
| hm        | 7.5                   | 85.8                          | 0.4                              | -21.5                   | -16.1               | -1.0                             | -6.8            | 0.4                       | -1.3                              | -0.2         | -1.1                               |
| hm        | 10.0                  | 68.6                          | 2.1                              | -18.7                   | -13.8               | 0.1                              | -5.6            | 2.1                       | -1.1                              | -0.6         | -0.5                               |
| <b>hm</b> | <b>mean</b>           | <b>93.2</b>                   | <b>1.1</b>                       | <b>-23.1</b>            | <b>-14.3</b>        | <b>-0.4</b>                      | <b>-7.2</b>     | <b>1.1</b>                | <b>-0.8</b>                       | <b>-0.2</b>  | <b>-0.6</b>                        |

**Table 1:** Sensitivity of textural parameters to a 40% reduction in ventilated lung volume. The latter was achieved by randomly inserting black cubes of side length 2.5, 5, 7.5 and 10mm into the simulated lung. Results are shown as relative changes in the textural parameter for either preparing the data in a histogram-matched (hm) or a contrast-stretched (cs) way and as a mean over 5 distances used in the GLCM calculation.

| Histogram | TC 1<br>Angular<br>Second<br>Moment | TC 3<br>Inverse<br>Different<br>Moment | TC 4<br>Diagonal<br>Moment | TC 9<br>Corre<br>lation | TC18<br>Coefficient<br>of<br>Variation | TC21<br>Entro<br>py | TC30<br>Local<br>Homog<br>eneity | TC13<br>Sum of<br>squares<br>(Variance) | TC31<br>Mean | TC13/<br>TC31<br>Variance<br>/Mean<br>ratio |
|-----------|-------------------------------------|--|----------------------------|-------------------------|--|---------------------|----------------------------------|---|--------------|---|
| cs        | -62.6                               | -2.9                                   | 53.4                       | 10.8                    | -10.8                                  | 11.5                | -2.9                             | 8.7                                     | 10.4         | -1.5  |
| hm        | -62.3                               | -3.9                                   | 48.5                       | 9.0                     | 0.5                                    | 11.3                | -3.9                             | -0.1                                    | -0.3         | 0.2   |

**Table 2:** Sensitivity of textural parameters to a 40% increase in gamma counts. The simulated defects have a cube side length of 10mm. Listed are the differences in the values of the textural parameters derived from either the standard simulation with 40% NVV and associated drop in average brightness and an alternative simulation with a higher gamma count such that after knocking out 40% of the ventilated volume the IOD matched the IOD of the perfectly ventilated lung simulation.

## Figure captions

**Figure 1:** Illustration of textural parameter TC18, Coefficient of Variation, from the simulation study for cube-shaped defects of size 7.5mm cube side length as a function of non-ventilated lung volume in percent. The GLCMs were created for 5 pixel distances each (1, 2, 4, 8, 12 pixels) corresponding to distances in the lung of 4.7, 9.3, 18.7, 37.3 and 56.0mm, respectively. The coefficient of variation is larger for small pixel distances and increases with NVV and more rapidly so for larger defects (not illustrated).

**Figure 2:** Relative ventilated lung volume (solid black) and standard variation (hashed) per patient group.

**Figure 3:** Illustration of textural parameter TC18, the Coefficient of Variation, for a set of 5 'normal' lungs (left) and a set of 5 lungs of patients suffering from COPD (right). The severity of COPD increases from top to bottom.

**Figure 4:** Textural parameter 18 (solid black) and standard deviation (hashed) from the invariant GLCM and for all 5 distances for the 5 patient groups studied

**Figure 5:** Ratio of textural parameter 30/31 (solid black) and standard deviation (hashed) from the invariant GLCM and mean over 5 distances for the 5 patient groups studied

**Figure 6:** High correlation between ventilated lung volume in percent and textural parameter 18 (coefficient of variation) ( $r^2=0.955$ ).

**Figure 7:** Correlation between textural parameter TC13/TC31 (Variance over Mean ratio) and independent spirometry data (FeV1) for 4 of the 5 patient groups. No spirometry data was available for the 'normal' group. The quality of the linear regression is  $r^2=0.66$ .

FIGURE 1

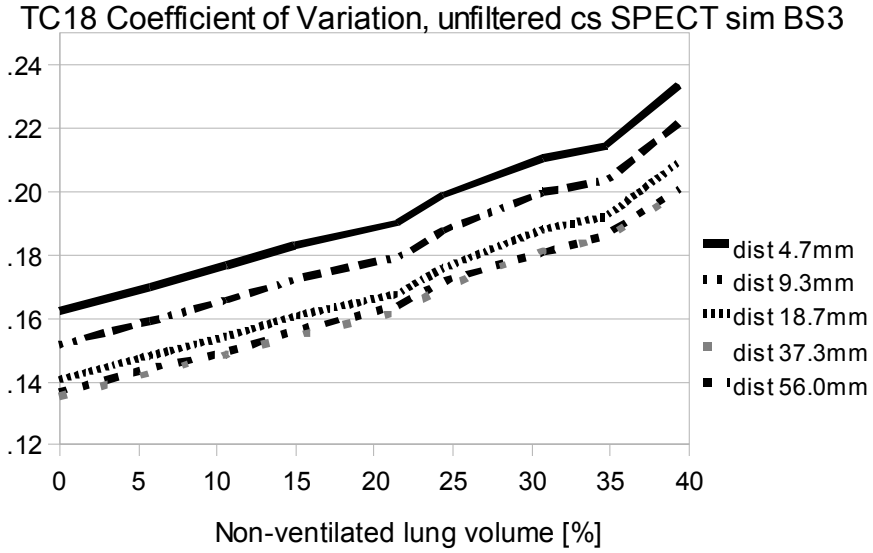


FIGURE 2

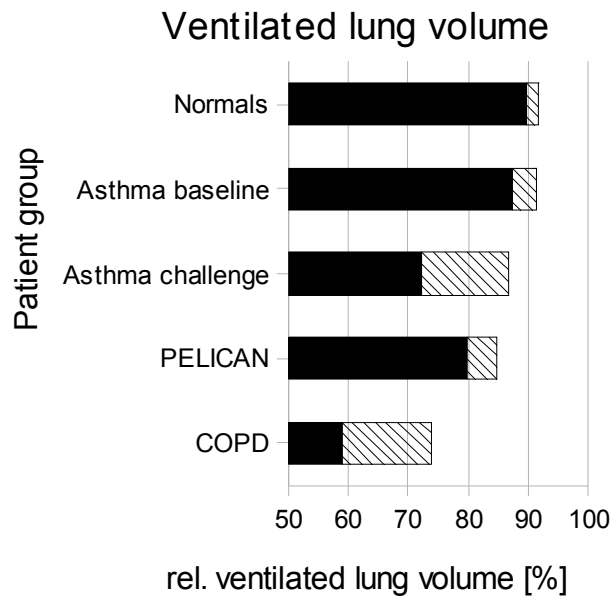


FIGURE 3 (left and right panel, reproduction in black-and-white)

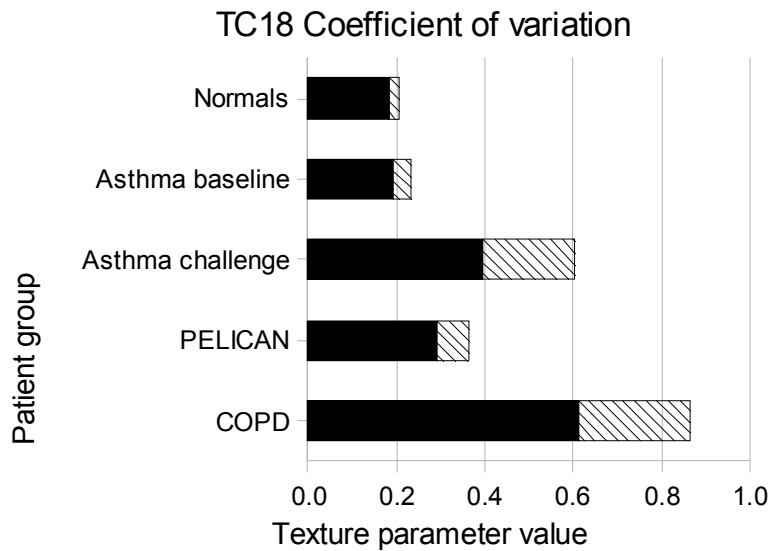
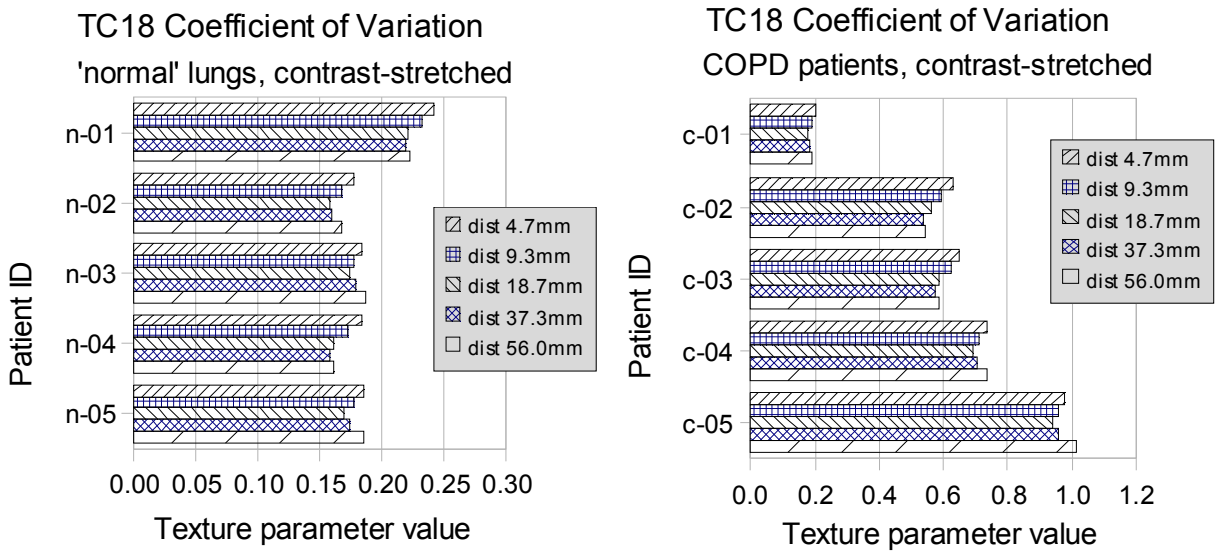


FIGURE 4

FIGURE 5

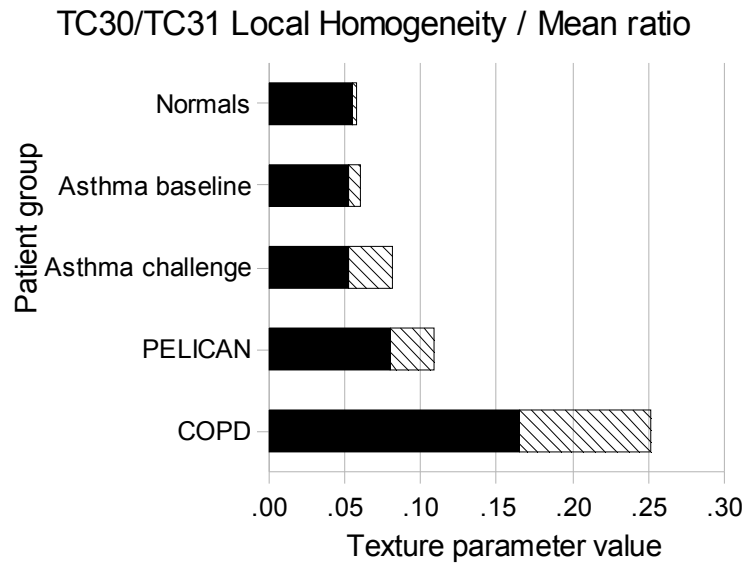


FIGURE 6 (colour reproduction for web-publishing, black-and-white for print)

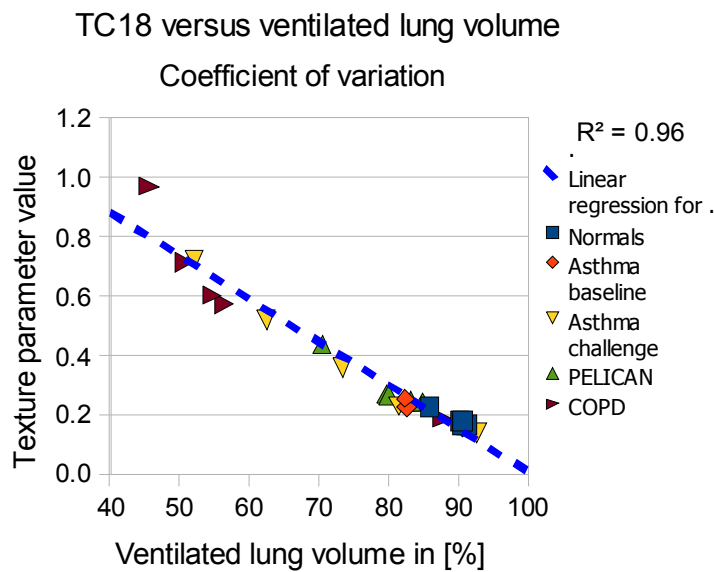
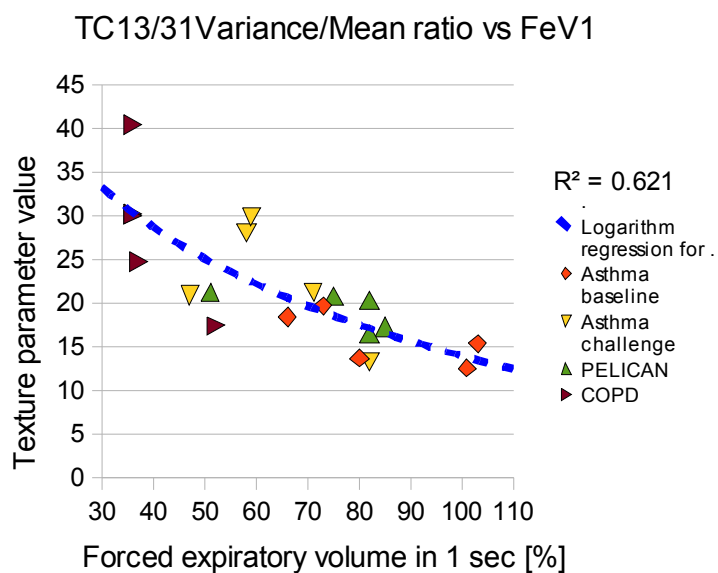




FIGURE 7 (colour reproduction for web-publishing, black-and-white for print)



Sydney, 8 December, 2008

Dr Arndt Meier  
Electron Microscope Unit  
Australian Key Centre for Microscopy and Microanalysis  
Madsen Bldg F09, Room 270  
Sydney University NSW 2006, AUSTRALIA

phone +61 2 9036 6417  
fax +61 2 9351 7682  
a.meier@usyd.edu.au  
[www.emu.usyd.edu.au](http://www.emu.usyd.edu.au)

To:  
The editor  
Computerized Medical Imaging and Graphics

Dear editor,

we are submitting the manuscript

### **Application of Texture Analysis to Functional Pulmonary CT Data**

Arndt Meier<sup>a</sup>, Catherine Walsh<sup>b,c,d</sup>, Benjamin E. Harris<sup>b,c,d</sup>, Gregory G.King<sup>b,c,d</sup>, and Allan Jones<sup>a</sup>

- a) Australian Key Centre for Microscopy and Microanalysis, The University of Sydney, Sydney 2006, NSW, Australia, email: [a.meier@usyd.edu.au](mailto:a.meier@usyd.edu.au) (*corresponding author*)
- b) Department of Respiratory Medicine, Royal North Shore Hospital, St Leonards NSW 2065
- c) Woolcock Inst. of Medical Research, 431 Glebe Point Road, Glebe, NSW 2037
- d) Northern Clinical School, Faculty of Medicine, University of Sydney, Sydney, 2006

for publication in the journal Computerized Medical Imaging and Graphics. The work is new and genuine and has not been published previously in this or any other form nor has it been submitted to any other publisher. All studies involving human subjects have been conducted in accordance with international and local ethics requirements.

This statement is made on behalf of all authors of the manuscript.

The manuscript was prepared in OpenOffice and then exported to MS Word data format. We are additionally sending a copy in PDF format as a 'ground-truth' in the unlikely event that tables or formulas look corrupted after importing the manuscript into a genuine MS Office application. Please notify us should this happen so we can fix any problems.

We believe that the material presented is of interest to your readers and that it has been prepared in a diligent way and that it meets all criteria for submission. We are happy to clarify any questions you or the reviewers may have.

Kind Regards,

Arndt Meier